Stereochemistry of selenium- and tellurium-bridged heteromerous bistricyclic aromatic enes. The fluorenylidenechalcoxanthene series

Amalia Levy, P. Ulrich Biedermann, Shmuel Cohen and Israel Agranat *

Department of Organic Chemistry, The Hebrew University of Jerusalem, Jerusalem, 91904, Israel. E-mail: isria@vms.huji.ac.il

Received (in Cambridge, UK) 4th June 2001, Accepted 22nd August 2001
First published as an Advance Article on the web 2nd November 2001

The effects of selenium and tellurium bridges on the conformations and dynamic stereochemical behavior of heteromerous bistricyclic aromatic enes (**1**) were studied. 9-(9′*H*-Fluoren-9′-ylidene)-9*H*-selenoxanthene (**9**) and 9-(9′*H*-fluoren-9′-ylidene)-9*H*-telluroxanthene (**10**) were synthesized, applying Barton's two-fold extrusion diazo–thione coupling method, which is especially suited for heteromerous **1**. The isopropyl derivatives **14**, **15** and the benzannulated derivatives **16**, **17**, and **18** were prepared analogously. The structures of **9**, **10**, **14**, **15**, and **16**–**18** were established by ^{1}H, ^{13}C, ^{77}Se, and ^{125}Te NMR spectroscopy and in the cases of **9** and **10** also by X-ray analysis. The molecules of **9** and **10** adopted *anti*-folded and folded conformations with 56.3/62.0° and 10.2/8.0° (**9**) and 63.6 and 2.2° (**10**) folding dihedrals, higher than in **7** and **8**. The degrees of pyramidalization of C^{9} and C$^{9'}$ were 2.8/3.9° and 0.9/2.1° (**9**) and 8 and 15° (**10**). Considerable overcrowding was evident in the short Se^{10} ··· C^{9} and Te^{10} ··· C^{9} contact distances in **9** and **10**. The crystal structures of **10** indicated relatively short intermolecular Te ··· Te distances (408 pm). The ^{13}C NMR chemical shifts of **9**, **10**, 9-(9′*H*-fluoren-9′-ylidene)-9*H*-xanthene (**12**) and 9-(9′*H*-fluoren-9′-ylidene)-9*H*-thioxanthene (**13**) indicated a variation in C^{9} of the chalcoxanthenylidene moiety, ascribed to through space interactions of Se, Te and S with C^{9}. The ^{77}Se and ^{125}Te NMR signals of **9**–**10** and **14**–**17** were shifted downfield relative to the homomerous **7** and **8**. A DNMR study of **14** and **15** gave $\Delta G_c^{\ddagger}$ (conformational inversion) = 14.4 (**14**) and 19.4 kcal mol^{-1} (**15**) and $\Delta G_c^{\ddagger}$ (*E*,*Z*-topomerizations) > 21.6 kcal mol^{-1}, indicating an increase of $\Delta G_c^{\ddagger}$ in the fluorenylidenechalcoxanthenes series (**11**): O < S < Se < Te. The fluorenylidene-derived **1** were found to show distinct behavior for conformational inversions and *E*,*Z*-isomerizations. Semiempirical PM3 calculations of **9** and **10** indicated that unevenly *anti*-folded conformations were most stable. Conformational inversions of **9** and **10** proceed *via* the twisted transition states corresponding to calculated barriers of 14.8 and 21.6 kcal mol^{-1} in excellent agreement with experiment. The *E*,*Z*-isomerizations proceed *via* orthogonally twisted biradical transition states with predicted barriers of 27.0 and 34.0 kcal mol^{-1} for **9** and **10**, respectively.

Introduction

The bistricyclic aromatic enes (**1**) have fascinated chemists since bifluorenylidene (**2**) and dixanthylene † (**3**) were synthesized and thermochromism was revealed in bianthrone † (**4**).[1–5] They can be classified into homomerous bistricyclic enes (**1**, X = Y) and heteromerous bistricyclic enes (**1**, X ≠ Y).[3,6] The bistricyclic enes are overcrowded in the fjord regions.[4] There are two principal modes of out-of-plane deformation in **1**: twisting around the central double bond (C^{9}=C$^{9'}$) and out-of-plane bending.[3,4] The bending is realized by folding of the tricyclic moieties.[3,4,7] In addition, C^{9} and C$^{9'}$ may be pyramidalized.[1–4] The nonplanarity of **1** may introduce chirality.[4,6] The major mode of deviation from planarity is strongly dependent on the sizes of the central rings and on the bridges X, Y (bond lengths C–X and C–Y, distances C^{4a} ··· C^{10a}).[3,8,9] A variety of conformations have been revealed in the homomerous bistricyclic enes, including twisted bifluorenylidene[10,11] (**2**), *anti*-folded dixanthylene[12] (**3**), *anti*-folded bianthrone[13] (**4**), and *anti*-folded and *syn*-folded 5,5′-bi(5*H*-dibenzo[*a*,*d*]cyclohepten-5-ylidene)[14] (**5**). A schematic representation of overall molecular shapes of bistricyclic enes is shown in Fig. 1. The dynamic processes of homomerous bistricyclic enes with central six-membered rings and of **2** have been extensively studied,[3,4,6,8,9,15–17] in contrast to the heteromerous bistricyclic enes, where attention has been mostly focused (*vide infra*) on sulfur-bridged **1**.[9]

† The IUPAC names for dixanthylene, bianthrone, dithioxanthylene and xanthone are bixanthenylidene, [bianthracene]dione, bi(thioxanthenylidene) and xanthenone, respectively.

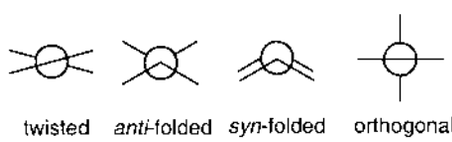

Fig. 1 Schematic projection along C^{9}=C$^{9'}$ of various conformations of bistricyclic enes (lines represent the peripheral benzene rings of the moieties).

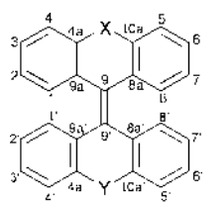

1, X = Y *homomerous*
1, X ≠ Y *heteromerous*

In the series of homomerous chalcogeno-bridged bistricyclic enes (**1**, X = Y = O, S, Se, Te), until very recently, only dixanthylene[12,16] (**3**) and dithioxanthylene †[9,18] (**6**) have been studied.[3,4] Last year we reported the results of a study of the selenium- and tellurium-bridged homomerous bistricyclic enes 9,9′-bi(9*H*-selenoxanthen-9-ylidene) (**7**) and 9,9′-bi(9*H*-telluroxanthen-9-ylidene) (**8**).[19] These molecules adopted *anti*-folded conformations with 53.6° (**7**) and 53.1° (**8**) folding dihedrals between pairs of benzene rings of the tricyclic moieties and showed low degrees of overcrowding in the fjord regions.[19] The present

DOI: 10.1039/b104858a

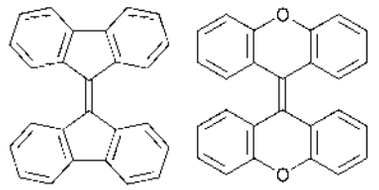

2 **3**

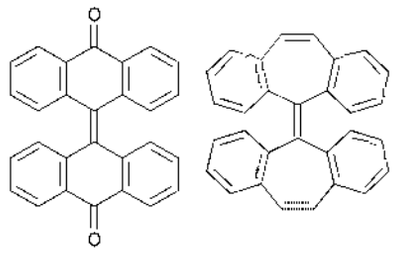

4 **5**

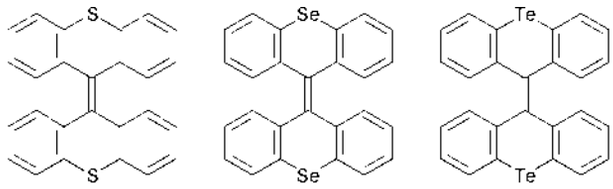

6 **7** **8**

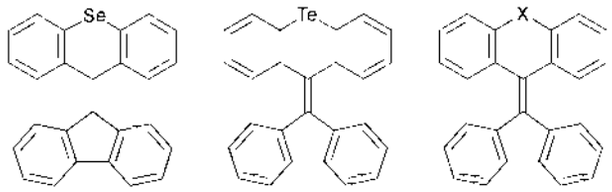

9 **10** **11** (X= O. S. Se. Te)

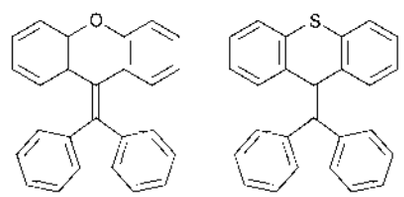

12 **13**

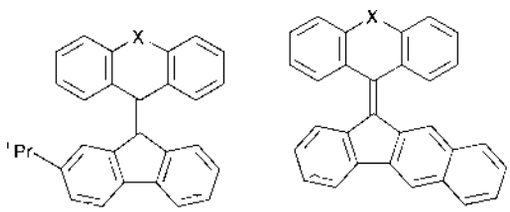

14, X= Se
15, X= Te

16, X=Se **17**, X=Te
18, X=S **19**, X=O

article describes the syntheses, molecular and crystal structures, NMR spectra, semiempirical calculations and a DNMR study of selenium- and tellurium-bridged heteromerous bistricyclic enes with central five-membered and six-membered rings, 9-(9′*H*-fluoren-9′-ylidene)-9*H*-selenoxanthene (**9**) and 9-(9′*H*-fluoren-9′-ylidene)-9*H*-telluroxanthene (**10**) and related derivatives. These systems belong to the fluorenylidenechalcoxanthene series (**11**). The competition between twisting and folding intensifies in heteromerous bistricyclic enes with central five- and six-membered rings. The fluorenylidene moiety has an energetic propensity against folding, contrary to the chalcoxanthenylidene moieties, including selenoxanthenylidene and telluroxanthenylidene. Moreover, **11**, in principle, is a potential push–pull system with its fluorenylidene and chalcoxanthenylidene moieties serving as acceptor and donor, respectively. Very recently we reported on the interplay between twisting and folding in the conformational space of 9-(9′*H*-fluoren-9′-ylidene)-9*H*-xanthene (**12**).[20] 9-(9′*H*-fluoren-9′-ylidene)-9*H*-thioxanthene (**13**) was found to be *anti*-folded. It seemed of interest to find out how the selenium and tellurium bridges in **11**, with their elongated Se–C and Te–C bonds would affect the conformations and the dynamic stereochemistry of these heteromerous bistricyclic aromatic enes. The isopropyl derivatives of **9** and **10**, 9-(2′-(1″-methylethyl)-9′*H*-fluoren-9′-ylidene)-9*H*-selenoxanthene (**14**) and 9-(2′-(1″-methylethyl)-9′*H*-fluoren-9′-ylidene)-9*H*-telluroxanthene (**15**) were synthesized in order to carry out a DNMR spectroscopic study of the conformational behavior of these systems. The syntheses of 9-(11′*H*-benzo[*b*]fluorene-11′-ylidene)-9*H*-selenoxanthene (**16**), 9-(11′*H*-benzo[*b*]fluoren-11′-ylidene)-9*H*-telluroxanthene (**17**) and 9-(11′*H*-benzo[*b*]fluoren-11′-ylidene)-9*H*-thioxanthene (**18**) are also described. Compounds **16**–**18** were studied in order to evaluate the effect of benzannulation on the stereochemistry of the parent compounds **9**, **10**, and **13**. In 9-(11′*H*-benzo[*b*]fluoren-11′-ylidene)-9*H*-xanthene (**19**) there is a subtle equilibrium between the yellow *anti*-folded conformation and the thermochromic purple twisted conformation at ambient temperature.[20] Therefore, it was interesting to study the complete homologous 9-(11′*H*-benzo[*b*]fluoren-11′-ylidene)-9*H*-chalcoxanthene series, including **18**.

Results and discussion

Synthesis

The fluorenylidenechalcoxanthenes **9** and **10** were synthesized by applying Barton's two-fold extrusion diazo–thione coupling method.[21–23] In principle, both the diazofluorene–chalcoxanthenethione and the fluorenethione–diazochalcoxanthene couplings could be adopted. The former route was preferred, taking advantage of the relatively convenient preparations of the reactants, their stabilities (aromatic dipolar structures) and their reactivities as carbon nucleophiles and carbon electrophiles, respectively, in the diazo–thione couplings. The method is especially suited for the synthesis of heteromerous bistricyclic enes. The starting materials were the tricyclic ketones 9*H*-selenoxanthen-9-one[24,25] (**20**) and 9*H*-telluroxanthen-9-one[26,27] (**21**). 9*H*-Selenoxanthene-9-thione (**22**) and 9*H*-telluroxanthene-9-thione (**23**) were prepared from **20** and **21**, respectively, using Lawesson's reagent,[28–30] in boiling benzene, as previously described.[19] The diazo–thione coupling of 9-diazo-9*H*-fluorene[31] (**24**) with **22** and **23** in boiling benzene gave dispiro[9*H*-fluorene-9,2′-thiirane-3′,9″-(9″*H*-selenoxanthene)] (**25**) and dispiro[9*H*-fluorene-9,2′-thiirane-3′,9″-(9″*H*-telluroxanthene)] (**26**), respectively. Elimination of sulfur from **25** and **26** with triphenylphosphine in boiling benzene gave **9** and **10**, respectively (Scheme 1).

The isopropyl derivatives **14** and **15** were synthesized analogously by applying Barton's two-fold extrusion diazo–thione coupling between the thioketones **22** and **23** and 9-diazo-2-(1′-methylethyl)-9*H*-fluorene[32] (**27**) *via* the dispirothiiranes **28** and **29**. The introduction of the isopropyl substituent in the fluorenylidene moiety at position 2′ of **11** rather than in the chalcoxanthenylidene moiety was preferred, due to the convenience of synthesis. The scope of the chemistry of the selenium- and tellurium-bridged tricyclic aromatic ketones **20** and **21** is limited[33,34] and their isopropyl derivatives are not known, in contrast to the 2-isopropyl derivatives of fluorenone, xanthone,† and thioxanthone. Compounds **16**, **17**, and **18** were synthesized analogously to **9** and **10** by couplings of 11-diazo-11*H*-benzo[*b*]-fluorene (**30**) with **22**, **23**, and 9*H*-thioxanthene-9-thione[30] (**31**)

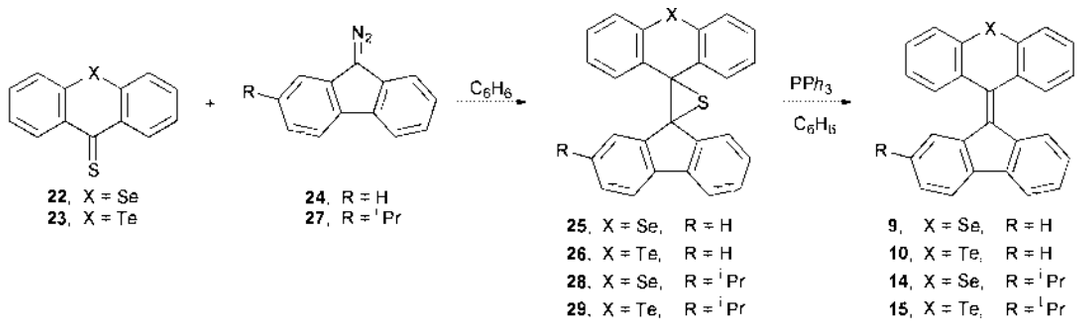

Scheme 1

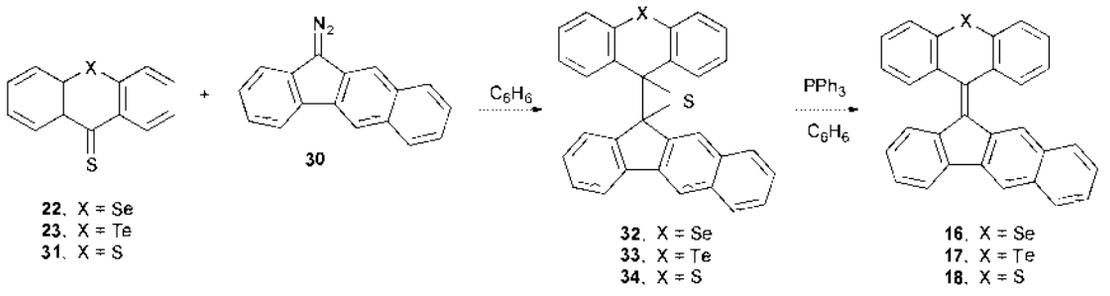

Scheme 2

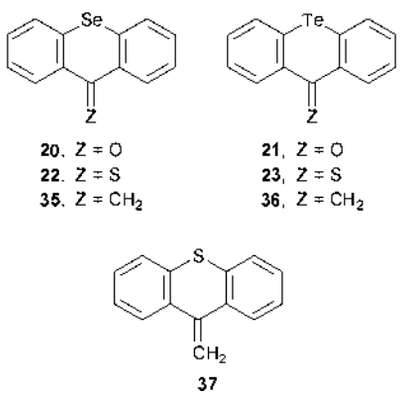

via the dispirothiiranes **32**, **33**, and **34** (Scheme 2). Compound **30** was prepared from 11*H*-benzo[*b*]fluoren-9-one[35] in two steps by conversion to the hydrazone, followed by oxidation, using HgO. Treatment of the dispirothiiranes **32**–**34** with triphenylphosphine in boiling benzene gave **16**, **17** and **18**, respectively. Elimination of sulfur from **34** to give **18** was also effected by copper in boiling xylene.

Molecular and crystal structures

The crystal structures of bistricyclic aromatic enes (**1**) have recently been reviewed.[3] Among the chalcogeno-bridged members of this series, only the old crystal structures of **3**[12] and those of derivatives of dithioxanthylene and thioxanthylidenexanthene have been described until very recently.[36] Last year we reported the molecular and crystal structures of the homomerous **7** and **8**.[19] 9-(9′*H*-Fluoren-9′-ylidene)-9*H*-selenoxanthene (**9**) crystallized in the space group $P2_1/c$. There are two independent molecules of **9** in the unit cell, labeled **9a** and **9b**. Both molecules are in a general crystallographic position (C_1 symmetry), however, they are close to C_s symmetry. Corresponding bond lengths, angles and torsion angles have root-mean-square differences of 0.9 pm, 1.2 and 1.8°, respectively. 9-(9′*H*-Fluoren-9′-ylidene)-9*H*-telluroxanthene (**10**) crystallized in the space group C_2. The molecule has a crystallographic C_1 symmetry, but is close to C_s symmetry. The root-mean-square differences of symmetry related bond lengths, angles and torsion angles are 3 pm, 1.4 and 2.5°, respectively. Fig. 2 gives ORTEP diagrams of **9a** and **10** as determined by X-ray

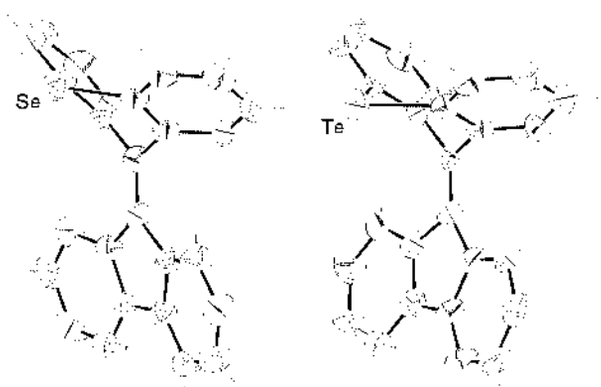

Fig. 2 ORTEP diagrams of the X-ray structures of **9a** (left) and **10** (right).

analysis. Table 1 gives the conformations and selected geometrical parameters of fluorenylidenechalcoxanthenes **9**, **10**, **12** and **13**, and the homomerous **7** and **8** derived from the crystal structures and/or from PM3 calculations (*vide infra*).

The overall conformations of the bistricyclic aromatic enes are characterized by the pure twist of the central C^9=$C^{9'}$ bond and by the folding dihedrals of the tricyclic moieties. The folding dihedral is defined as the dihedral angle of the least-squares-planes of the carbons C^1, C^2, C^3, C^4, C^{4a}, C^{9a} and C^5, C^6, C^7, C^8, C^{8a}, C^{10a} of the two benzene rings of a tricyclic moiety.[3] The pyramidalization angles χ_9 and $\chi_{9'}$ should also be considered.[3] The molecular and crystal structures of **9** and **10** indicated that **9** adopts an *anti*-folded conformation with uneven degrees of folding (**au-9**) and that **10** adopts a (mono-) folded conformation (**f-10**), in contrast to the twisted **12** (**t-12**).[20] The folding dihedrals in the selenoxanthenylidene moieties of **9a** and **9b** are 56.3 and 62.0°, respectively. The folding dihedrals in the fluorenylidene moieties of **9a** and **9b** are 10.2 and 8.0°, respectively. The selenoxanthenylidene and fluorenylidene moieties of **9** are folded in opposite directions. In the case of **10**, the folding dihedral in the telluroxanthenylidene moiety is 63.6°, while the folding dihedral in the fluorenylidene moiety is only 2.2°. Formally, the conformation of **10** is *syn*-folded, *i.e.*, both moieties are folded in the same direction.

Table 1 Conformations and selected geometrical parameters of **7**–**10**, **12**, and **13** derived from crystal structures and PM3 calculations

	X, Y	Method	Conformation[a]	Symmetry	Folding angle/°		Pure twist	$C^1 \cdots C^{1'}$/pm	$C^1 \cdots H^{1'}$/pm	$C^1 \cdots H^{1'}$/pm	$H^1 \cdots H^{1'}$/pm	$X^{10} \cdots C^9$/pm	$C^9{=}C^{9'}$/pm	C^{9a}–C^9–C^{8a}/°		χ_9/°	$\chi_{9'}$/°	C–X/pm	C–X–C /°	$C^{4a} \cdots C^{10a}$/pm
10	Te, —	X-Ray	**f**	C_1	63.6	2.2	0.5	325	248	331	265	315	135	111.0	105.0	8	15	212.4	88.1	295
10	Te, —	PM3	**au**	C_s	64.8	3.7	0.0	324	245	334	282	303	134.8	111.9	104.9	4.8	0.9	213.9	90.1	303
10	Te, —	PM3	**t**	C_2	26.3	3.4	41.4	298	259	268	272	351	137.9	124.0	104.8	0.0	0.0	210.6	92.2	303
10	Te, —	PM3	$\mathbf{t}_\perp$	C_{2v}	0.0	0.0	90.0	395	384	359	371	345	145.9	128.8	107.2	0.0	0.0	210.7	94.4	305
9a	Se, —	X-Ray	**au**	C_1	56.3	10.2	0.7	307	240	297	255	308	134.7	111.7	104.2	2.8	0.9	190.8	94.2	279
9b	Se, —	X-Ray	**au**	C_1	62.0	8.0	2.5	315	251	307	249	305	135.1	111.1	104.5	3.9	2.1	190.6	93.3	277
9	Se, —	PM3	**au**	C_s	59.6	7.6	0.0	314	241	312	270	297	134.9	111.1	104.7	5.1	1.6	188.9	95.5	280
9	Se, —	PM3	**t**	C_2	14.5	3.4	43.6	299	259	259	261	330	137.9	122.0	104.9	0.0	0.0	186.5	99.7	285
9	Se, —	PM3	$\mathbf{t}_\perp$	C_{2v}	0.0	0.0	90.0	400	387	357	374	323	145.6	125.8	107.3	0.0	0.0	186.5	100.4	287
13	S, —	PM3	**au**	C_s	53.9	10.3	0.0	306	238	297	264	301	135.0	110.4	104.5	5.7	2.7	176.9	98.0	267
13	S, —	PM3	**t**	C_2	12.5	3.3	43.7	300	259	257	258	322	137.8	120.2	104.9	0.0	0.0	174.1	102.9	272
13	S, —	PM3	$\mathbf{t}_\perp$	C_{2v}	0.0	0.0	90.0	401	387	358	374	316	145.5	123.8	107.3	0.0	0.0	173.9	103.3	273
12	O, —	PM3	**au**	C_s	46.3	14.9	0.0	299	236	273	247	279	135.1	108.4	104.3	7.2	5.3	139.2	111.4	230
12	O, —	PM3	**t**	C_2	5.2	2.5	41.4	304	257	250	243	292	137.2	114.8	105.1	0.0	0.0	137.7	116.8	235
12	O, —	PM3	$\mathbf{t}_\perp$	C_{2v}	0.0	0.0	90.0	412	394	372	382	287	144.7	117.9	107.3	0.0	0.0	137.9	116.8	235
8	Te, Te	X-Ray	**af**	C_i	53.1	53.1	0.0	324	327	327	356	323	134.9	115.2		1.7		211.4	89.3	297
8	Te, Te	PM3	**af**	C_{2h}	57.8	57.8	0.0	362	380	380	424	306	134.8	114.9		1.6		213.6	90.9	304
8	Te, Te	PM3	**sf**	C_{2v}	59.6	59.6	0.0	343	320	320	265	296	134.6	114.6		12.2		214.2	91.3	306
8	Te, Te	PM3	**t**	D_2	18.6	18.6	54.8	304	295	295	322	350	140.8	125.0		0.0		210.5	92.4	304
8	Te, Te	PM3	$\mathbf{t}_\perp$	D_{2d}	0.0	0.0	90.0	344	339	339	349	345	148.8	128.7		0.0		210.7	93.1	304
7	Se, Se	X-Ray	**af**	C_1	52.5	54.7	1.6	326	319	319	348	308	133.9	112.8		0.5		190.7	94.3	280
7	Se, Se	PM3	**af**	C_{2h}	51.6	51.6	0.0	330	337	337	375	302	135.1	114.0		2.2		188.5	96.5	281
7	Se, Se	PM3	**sf**	C_{2v}	54.8	54.8	0.0	303	257	257	178	301	135.1	112.5		7.4		188.6	95.9	280
7	Se, Se	PM3	**t**	D_2	8.6	8.6	56.1	302	280	280	299	329	140.6	122.6		0.0		188.5	99.9	286
7	Se, Se	PM3	$\mathbf{t}_\perp$	D_{2d}	0.0	0.0	90	371	345	345	352	323	148.0	125.7		0.0		186.7	100.5	287

[a] Conformation: **f**: folded; **au**: unevenly *anti*-folded; **t**: twisted; $\mathbf{t}_\perp$: orthogonally twisted; **af**: *anti*-folded; **sf**: *syn*-folded.

Table 2 ^{1}H NMR chemical shifts[a] (δ) of **2**, **3**, **6**–**10**, **12**, **13**

	X, Y	Conformation[b]	H^1, H^8 $H^{1'}$, $H^{8'}$	H^2, H^7 $H^{2'}$, $H^{7'}$	H^3, H^6 $H^{3'}$, $H^{6'}$	H^4, H^5 $H^{4'}$, $H^{5'}$
10	Te, —	**au**	7.733	7.344	7.198	8.004
			6.934	6.934	7.247	7.658
9	Se, —	**au**	7.778	7.330	7.257	7.823
			7.192	6.946	7.257	7.659
13	S, —	**au**	7.829	7.332	7.332	7.703
			7.358	6.975	7.273	7.547
12	O, —	**t**	8.134	7.124	7.360	7.366
			7.889	7.066	7.268	7.724
8	Te, Te	**af**	6.796	6.879	6.963	7.801
7	Se, Se	**af**	6.787	6.904	7.072	7.656
6	S, S	**af**	6.818	6.911	7.120	7.537
3	O, O	**af**	7.146	6.877	7.226	7.270
2	—, —	**t**	8.386	7.211	7.332	7.709

[a] In $CDCl_3$ (relative to $CHCl_3$ δ = 7.26 ppm). [b] Conformation: **au**: unevenly *anti*-folded; **t**: twisted; **af**: *anti*-folded.

However, due to the very small folding dihedral of the fluorenylidene moiety, the molecular structure of **10** may be better described as a conformation with one strongly folded moiety and one planar moiety (**f**). The degrees of folding in the chalcoxanthenylidene moieties of **9** and **10** were higher than those observed in the homomerous **7** and **8**. The molecular structures of **9** and **10** differ also in the degree of pyramidalization χ_9 and $\chi_{9'}$ of the central C^9=$C^{9'}$ bond. In **9a** and **9b**, χ_9 = 2.8 and 3.9°; $\chi_{9'}$ = 0.9 and 2.1°, respectively. The double bond of **9a** is *anti*-pyramidalized, while that of **9b** is *syn*-pyramidalized. The pyramidalization angles are only slightly higher than in **7** (0.5°). In **10**, the central double bond is *syn*-pyramidalized with χ_9 = 8° and $\chi_{9'}$ = 15°, as compared with 1.7° in **8**. The high degree of pyramidalization in **f-10** points at an additional mode for solving the overcrowding in the fjord regions when the fluorenylidene moiety is almost planar and the chalcoxanthenylidene moiety is highly folded (63.6°). Obviously, the molecular structures of **9** and **10** differ in the geometrical parameters pertaining directly to the chalcogen bridges. Thus, in **9**, C^{4a}–Se^{10}, C^{4a}–Se^{10}–C^{10a} and $C^{4a} \cdots C^{10a}$ are 190.8 pm, 94.2 and 93.3°, and 279 and 277 pm, respectively, while in **10**, C^{4a}–Te^{10}, C^{4a}–Te^{10}–C^{10a}, and $C^{4a} \cdots C^{10a}$ are 212.4 pm, 88.1° and 295 pm, respectively. The degrees of overcrowding in the fjord regions of **9a** and **9b** as reflected in the intramolecular nonbonding distances between the fjord region carbons and hydrogens, $C^1 \cdots C^{1'}$, $C^1 \cdots H^{1'}$ and $H^1 \cdots H^{1'}$ are relatively high, especially in **9a**: $C^1 \cdots C^{1'}$ = 307 (**9a**), 315 (**9b**) pm, $C^1 \cdots H^{1'}$ = 240 (**9a**), 251 (**9b**) pm, and $H^1 \cdots H^{1'}$ = 255 (**9a**), 249 (**9b**) pm. For comparison, the van der Waals radii of carbon and hydrogen are 171 and 115 pm,[37] respectively, resulting in van der Waals contact distances of 343, 286, and 230 pm, respectively. Thus, the penetrations in **9a** and **9b** are up to 16 and 12%. In **10**, the $C^1 \cdots C^{1'}$, $C^1 \cdots H^{1'}$, $H^1 \cdots H^{1'}$ nonbonding distances are 325, 248, and 265 pm, respectively, so that the penetration is up to 13%. The central C^9=$C^{9'}$ bond lengths of **9** and **10** are in the range 134.7–135.1 pm, slightly longer than in **7** (133.9 pm) and similar to **8** (134.9 pm). The $Se^{10} \cdots C^9$ nonbonding distances in **9a** and **9b** are 308 and 305 pm, respectively, while in **10**, the $Te \cdots C^9$ nonbonding distance is 315 pm. These distances are significantly shorter than the van der Waals contact distances Se ··· C 361 pm and Te ··· C 379 pm.[37,38] For comparison, in **7** and **8**, the corresponding nonbonding distances are 308 and 323 pm, respectively.[19] The short $X \cdots C^9$ nonbonding distances in **9** and **10** indicate an additional effect of intramolecular overcrowding in folded bistricyclic enes. The short $Te^{10} \cdots C^9$ distance of 315 pm may be due to the 10° higher degree of folding in **10** as compared with **8**. Indeed, in 9*H*-telluroxanthen-9-one (**21**), in which the folding dihedral is only 6.6°, the $Te^{10} \cdots C^9$ distance is significantly longer than in **10**, 349 pm.[39] The crystal structure of **10** indicates relatively short intermolecular Te ··· Te distances between the tellurium atom of one molecule and the tellurium atoms of two neighboring molecules: 408 pm. This value is very close to the Te ··· Te van der Waals contact distance, 416 pm.[38] The Te atoms form zigzag chains with a Te ··· Te ··· Te angle of 86°. A fragment of such a zigzag chain and the herringbone packing of the molecules are shown in Fig. 3. In the case of the crystal structure of **9**, the closest intermolecular Se ··· Se distance, 583 pm, appears between the selenium atoms of the two independent molecules in the unit cell. It is substantially longer than the Se ··· Se van der Waals contact distance, 380 pm.[38] The selenium atom is oriented towards the C^4–C^{4a}–C^{4b}–C^5 "bay region" of a fluorenylidene moiety of a neighboring molecule.

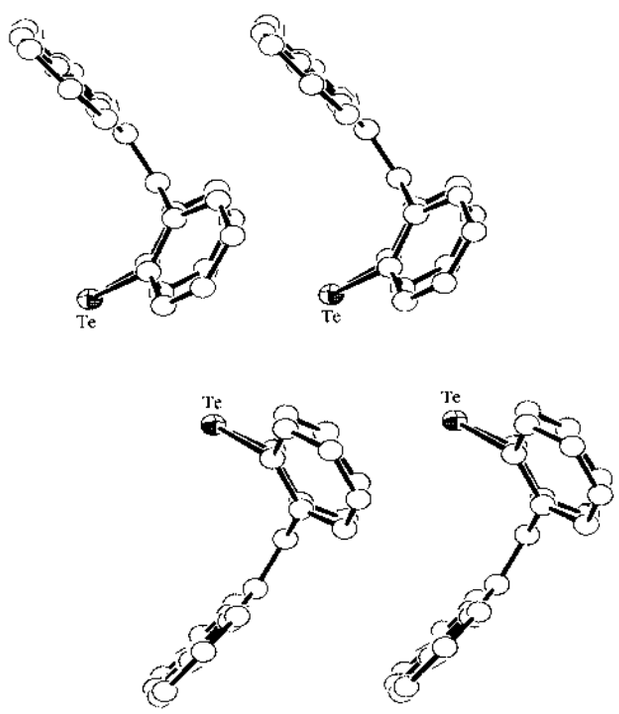

Fig. 3 Zigzag chain of Te atoms and herringbone type packing in the X-ray structure of **10**.

NMR Spectroscopy

^{1}H, ^{13}C, ^{77}Se, and ^{125}Te NMR spectroscopic studies of fluorenylidenechalcoxanthenes were carried out. Table 2 gives the ^{1}H NMR chemical shifts of fluorenylidenechalcoxanthenes (**11**) and related homomerous bistricyclic enes. Table 3 gives the ^{1}H NMR chemical shifts of benzo[*b*]fluorenylidenechalcoxanthenes and related compounds. Table 4 gives the ^{13}C NMR chemical shifts of **2**, **3**, **6**–**10**, **12**, and **13**. Table 5 gives the ^{77}Se

Table 3 Selected ^{1}H NMR chemical shifts[a] (δ) of **16**–**19**, and related compounds

	X, Y	Conformation[b]	$H^{5'}$	$H^{10'}$		$H^{1'}$, $H^{8'}$	$\Delta\delta$[c] (ppm)
17	Te, —	**au**	8.045	7.342	**10**	6.912	0.43
16	Se, —	**au**	8.051	7.637	**9**	7.192	0.44
18	S, —	**au**	8.068	7.832	**13**	7.358	0.47
19	O, —	**t**	8.110	8.410	**12**	7.889	0.52
[d]	—, —	**t**	8.131	8.900	**2**	8.368	0.52
[e]	—, —	**t**	8.142	9.120	**2**	8.368	0.72

[a] In $CDCl_3$ (relative to $CHCl_3$ δ = 7.26 ppm). [b] Conformation: **au**: unevenly *anti*-folded; **t**: twisted. [c] $\Delta\delta = \delta(H^{10'}) - \delta(H^{1'})$. [d] (*E*)-Bi(11*H*-benzo[*b*]fluoren-11-ylidene). [e] (*Z*)-Bi(11*H*-benzo[*b*]fluoren-11-ylidene).

Table 4 ^{13}C NMR chemical shifts[a] (δ) of **2**, **3**, **6**–**10**, **12**, and **13**

	X, Y	C^1, C^8 $C^{1'}$, $C^{8'}$	C^2, C^7 $C^{2'}$, $C^{7'}$	C^3, C^6 $C^{3'}$, $C^{6'}$	C^4, C^5 $C^{4'}$, $C^{5'}$	C^{4a}, C^{10a} $C^{4a'}$, $C^{10a'}$	C^{8a}, C^{9a} $C^{8a'}$, $C^{9a'}$	C^9 $C^{9'}$
10	Te, —	129.10	127.57	127.16	136.99	118.94	142.39	145.74
		125.65	126.36	128.26	119.31	140.90	137.96	131.37
9	Se, —	129.30	126.60	127.25	131.23	133.55	136.61	140.33
		125.59	126.22	128.25	119.33	140.94	137.99	131.55
13	S, —	129.03	126.12	127.30	128.68	136.53	137.29	137.29
		125.54	126.07	128.32	119.34	140.98	138.07	131.65
12	O, —	130.0	122.79	129.93	117.63	154.02	124.80	130.86
		124.27	125.85	127.44	119.43	140.28	139.34	130.99
8	Te, Te	130.67	127.02	126.57	134.98	118.01	141.27	143.69
7	Se, Se	130.47	126.18	126.68	129.47	132.42	137.44	137.44
6	S, S	129.85	125.73	126.72	127.10	135.65	135.99	133.59
3	O, O	128.31	122.40	128.12	117.08	155.48	124.92	121.44
2	—, —	126.73	126.85	129.15	119.89	141.31	138.28	141.01

[a] In $CDCl_3$ (relative to $CDCl_3$ δ = 77.01 ppm).

and ^{125}Te NMR chemical shifts of **7**–**10** and related compounds. Complete assignments were made through 2-dimensional correlation spectroscopy [COSY, heteronuclear single quantum coherence (HSQC), heteronuclear multiple bond coherence (HMBC)]. It is possible to distinguish qualitatively between the twisted conformation, the *anti*-folded conformation, and the *syn*-folded conformation of homomerous **1** in solution, using ^{1}H NMR chemical shifts of the fjord protons H^1, H^8, $H^{1'}$, $H^{8'}$.[19] In heteromerous **1**, the picture is somewhat more complicated. In **9**, **10** and **13**, the fjord region protons of the chalcoxanthenylidene moiety, H^1 and H^8, appear at 7.778, 7.733, and 7.829 ppm, respectively, while the corresponding protons of the fluorenylidene moiety, $H^{1'}$ and $H^{8'}$ appear at 7.192, 6.934 and 7.358 ppm, respectively. The difference in the chemical shifts of $H^{1'}$, $H^{8'}$ (fluorenylidene moiety) is wider than in that of H^1, H^8 (chalcoxanthenylidene moiety): *e.g.*, δ(**13**) − δ(**10**) = 0.096 and 0.424 ppm for H^1, H^8 and $H^{1'}$, $H^{8'}$, respectively. In **9**, **10** and **13**, the fjord region protons $H^{1'}$ and $H^{8'}$ are affected by the ring currents of the folded chalcoxanthenylidene moiety. The effect is more pronounced in **10**, in which the degree of folding of the telluroxanthenylidene moiety is higher and the fluorenylidene moiety is almost planar. However, the fjord region protons H^1 and H^8 of the chalcoxanthenylidene moiety are hardly affected by the aromatic rings of the opposing fluorenylidene moiety, which are only moderately folded (**9**) or almost planar (**10**). Therefore, H^1 and H^8 appear at lower aromatic field, as compared with the corresponding protons of the homomerous bistricyclic enes **6**–**8**. The ^{1}H NMR spectra of the benzo[*b*]-fluorenylidenechalcoxanthenes (Table 3) are complicated; therefore, full assignments of the spectra were not possible. Nevertheless, the benzo[*b*]fluorene singlets due to $H^{5'}$ and $H^{10'}$ have been identified. The chemical shifts of the fjord region $H^{10'}$ were compared to the chemical shifts of the fluorene fjord regions $H^{1'}$ and $H^{8'}$. Thus, for **16**, **17** and **18** *versus* **9**, **10** and **13**, $\delta(H^{10'}) - \delta(H^{1'})$ = 0.43–0.47 ppm. This rather constant difference is probably due to the effect of the naphthalene moiety in **16**, **17**, **18**. It is concluded that benz[*b*]annulation does not alter significantly the *anti*-folded conformations of the fluorenylidene-chalcoxanthenes. The shift to a lower field of $H^{5'}$, as compared with $H^{10'}$ is due to the fact that $H^{10'}$ is positioned above or below the benzene rings of the chalcoxanthenylidene moiety, while $H^{5'}$ is positioned farther away from the fjord regions.

The ^{13}C NMR chemical shifts of **9**, **10**, and **13** (Table 4) indicate a variation in C^9 of the chalcoxanthenylidene moiety: 145.74 (**10**), 140.33 (**9**), 137.29 ppm (**13**). For comparison, in the homomerous **1** the C^9 chemical shifts are 143.69 (**8**), 137.44 (**7**), and 133.59 ppm (**6**).[19] There are only slight variations in $C^{9'}$ of the fluorenylidene moiety: 131.37 (**10**), 131.55 (**9**), 131.65 (**13**). The above variations are ascribed to through space interactions of the bridges tellurium, selenium and sulfur with the sp^2 hybridized C^9: Te ··· C^9, Se ··· C^9, S ··· C^9. The chemical shifts of C^9 in the heteromerous **9**, **10**, and **13** are shifted downfield, as compared with the homomerous **8**, **7**, and **6**. The differences δ(**10**) − δ(**8**) = 2.05 ppm, δ(**9**) − δ(**7**) = 2.89 ppm and δ(**13**) − δ(**6**) = 3.70 ppm, may be due to a certain (small) contribution of dipolar structures in the heteromerous compounds. There are hardly any variations in the chemical shifts of the fjord regions C^1 and C^8 of the chalcoxanthenylidene moieties and $C^{1'}$ and $C^{8'}$ of the fluorenylidene moieties of **10**, **9** and **13**. Comparing the ^{13}C chemical shifts of the fluorenylidenechalcoxanthenes with the chemical shifts of the corresponding homomerous enes, small but systematic variations are observed. The aromatic fluorenylidene carbons in **9**, **10**, and **13** are shifted up-field by −0.3 to −1.3 ppm relative to the corresponding atoms in bifluorenylidene (**2**). On the other hand, the aromatic chalcoxanthene carbons in **9**, **10**, and **13** (with the exception of C^1, C^8) are shifted downfield by 0.3 to 2.0 ppm relative to the corresponding atoms in **7**, **8** and **6**, respectively. Since the chemical shift of carbon atoms correlates with the charge of the atom, this trend may be indicative of a push–pull effect.

The ^{77}Se and ^{125}Te NMR chemical shifts of **9**–**10** and **14**–**17** (Table 5) were very helpful, due to their sensitivity, in monitoring the progress of the syntheses leading to these selenium- and tellurium-bridged heteromerous bistricyclic enes. The chemical shifts of the chalcogen atoms in the fluorenylidenechalcoxanthenes are shifted downfield, relative to those of the

Table 5 ^{77}Se and ^{125}Te NMR chemical shifts of bistricyclic enes and related compounds

Se Compd	X, Y	δ^{77}Se[a] (ppm)	$\Delta\delta$ (ppm)[b]	Te Compd	X, Y	δ^{125}Te[c] (ppm)	$\Delta\delta$ (ppm)[d]	δTe/δSe
20		334.7	0.0	**21**		473.4	0.0	1.40
9	Se, —	398.2	63.5	**10**	Te, —	620.9	147.5	1.56
14	Se, —	397.7	63.0	**15**	Te, —	619.2	145.8	1.55
16	Se, —	397.7	63.0	**17**	Te, —	619.2	145.8	1.55
7	Se, Se	366.3	31.6	**8**	Te, Te	574.1	73.7	1.49

[a] In $CDCl_3$ (relative to Me_2Se in $CDCl_3$).[43] [b] Relative to selenoxanthone. [c] In $CDCl_3$ (relative to Me_2Te in C_6D_6).[43] [d] Relative to telluroxanthone.

Table 6 Results of DNMR studies of **14**–**15**, and related compounds

Compd	X, Y	Solvent	Process	Probe	$\Delta\nu$/Hz	T_c/K	$\Delta G_c^{\ddagger}$/kcal mol^{-1}
14	Se, —	$CDCl_3$	Inversion	^{13}C, CH_3	29.4	287	14.4
14	Se, —	$(CDCl_2)_2$	Topomerization[a]	^{13}C, C^1/C^8	17.1	>416	>21.6
15	Te, —	$CDCl_3$	Inversion	^{13}C, CH_3	20.6	378	19.4
15	Te, —	$(CDCl_2)_2$	Topomerization[a]	^{13}C, C^1/C^8	17.8	>416	>21.6
[b]	S, —		Inversion				12.2
[c]	O, —	$CDCl_2F$	Enantiomerization[a]	^{13}C, CH_3	57	134	6.3
[c]	O, —	C_7D_8	Topomerization[a]	^{13}C, C^1/C^8	5.1	363.5	19.6
[d]	—, —		Enantiomerization[a]	^{13}C, CH_3	52.3	218	10.5
[e]	—, —		*E*,*Z*-Isomerization	^{1}H, CH_3			25.0

[a] *E*,*Z*-Topomerization. [b] 2-(1″-Methylethyl)-9-(9′*H*-fluoren-9′-ylidene)-9*H*-thioxanthene.[46] [c] 2-(1″-Methylethyl)-9-(9′*H*-fluoren-9′-ylidene)-9*H*-xanthene.[20] [d] 2-(1″-Methylethyl)-bi(9*H*-fluoren-9-ylidene).[32] [e] 2,2′-Dimethylbi(9*H*-fluoren-9-ylidene).[32]

homomerous dichalcoxanthenylidenes: δ^{77}Se = 398.2 (**9**), 397.7 (**14**, and **16**) and 366.3 (**7**), δ^{125}Te = 620.9 (**10**), 619.2 (**15**, and **17**) and 547.1 (**8**). Thus, $\Delta\delta^{77}$Se = δ(**9**) − δ(**7**) = 31.9 ppm and $\Delta\delta^{125}$Te = δ(**10**) − δ(**8**) = 46.8 ppm. The difference in δ^{125}Te/δ^{77}Se between the heteromerous **9** and **10** and the homomerous **7** and **8** should also be noted: 1.56 *versus* 1.49. We have tentatively ascribed the deshieldings of δ^{77}Se and δ^{125}Te in the homomerous **7** and **8** (compared with their corresponding tricyclic systems), to an effect of the ring currents of the opposing aromatic rings in the *anti*-folded conformations and/or to the interactions of the selenium and tellurium atoms with the nonpolar C^9=$C^{9'}$ bonds in **7** and **8**. The enhanced deshielding effect in **9** and **10** relative to **7** and **8** is probably due to the higher folding dihedrals of the chalcoxanthenylidene moieties and to the higher degrees of overcrowding in **9** and **10**. The larger δ^{125}Te/δ^{77}Se ratio in **9** and **10** relative to **7** and **8** may be due not only to variations in the degree of folding, but also to the nonbonding interaction between Te and the pyramidalized C^9 in **10**. The results of the ^{77}Se and ^{125}Te NMR spectra strengthen the conclusion that these chemical shifts in selenium- and tellurium-bridged bistricyclic aromatic enes are conformation dependent.[40]

Dynamic NMR spectroscopy

In bistricyclic enes, three fundamental processes were observed:[3,4,8] (a) *E*,*Z*-isomerization (*e.g.*, $\mathbf{t}_E \rightleftharpoons \mathbf{t}_Z$, $\mathbf{af}_E \rightleftharpoons \mathbf{af}_Z$); (b) enantiomerization or conformational inversion, *i.e.*, inversion of the helicity in twisted **1** ($\mathbf{t}_P \rightleftharpoons \mathbf{t}_M$), or inversion of the boat conformation in the central rings of folded **1**; (c) *syn*, *anti* isomerization (**sf** $\rightleftharpoons$ **af**). It should be noted that enantiomerization and racemization may also be involved in processes (a) and (c).[3,8]

The DNMR studies of homomerous **1** revealed low barriers for thermal *E*,*Z*-isomerization ($\Delta G_c^{\ddagger}$ = 17–28 kcal mol^{-1}).[3,4,8,9,15–17] These remarkably low energy barriers were interpreted predominantly in terms of ground state destabilization due to steric strain and overcrowding rather than in terms of stabilization of biradical transition states. Feringa *et al.* have shown that for the series of substituted bistricyclic aromatic enes **1**: X = S; Y = S, $C(CH_3)_2$, $N(CH_3)_2$, O, the racemization barrier decreases: $\Delta G_c^{\ddagger}$ = 27.4, 25.1, 21.3, and 20.0 kcal mol^{-1} respectively.[9] It has been argued that the racemization barriers depend on the bridges X and Y, on the C–X and C–Y bond lengths and on the $C^{4a} \cdots C^{10a}$ distances.[8,9] The dynamic stereochemistry of 2-(1″-methylethyl)-9-(9′*H*-fluoren-9′-ylidene)-9*H*-xanthene has recently been reported.[20] The synthesis of the isopropyl derivatives **14** and **15** allowed a DNMR spectroscopic study of the conformational inversions and *E*,*Z*-topomerizations of these selenium- and tellurium-bridged heteromerous **11**. These derivatives are chiral, both in their twisted conformations and in their *anti*-folded conformations; only the orthogonally twisted and planar conformations are achiral. The conformational inversions of **14** and **15** were studied in the temperature ranges 217–315 K (**14**) and 280–384 K (**15**). The prochiral methyl groups of **14** appear in the ^{1}H NMR spectrum (in $CDCl_3$) at 298 K as a broad absorption at δ = 1.086 ppm, indicating a dynamic process. Upon heating to 315 K, it turned into a doublet at δ = 1.088 ppm (J = 6.8 Hz). Upon cooling to 240 K, it turned into two sharp doublets at δ = 1.015 ppm (J = 6.9 Hz) and 1.002 ppm (J = 6.9 Hz). In the ^{13}C NMR spectrum (in $CDCl_3$) at 298 K, the methyl carbons appeared as a singlet at δ = 22.86 ppm, which upon cooling to 240 K, turned into two singlets at δ = 23.67 and 24.09 ppm. The prochiral methyl groups of **15** appeared in the ^{1}H NMR spectrum (in Cl_2DC–$CDCl_2$) at 298 K as two doublets at δ = 0.987 and 1.055 ppm. In the ^{13}C NMR spectrum at 298 K, the methyl carbons appeared as two singlets at 24.35 and 23.96 ppm. The dynamic experiments were carried out by cooling or heating each sample and monitoring the absorptions of the methyl carbons. Coalescence occurred at 287 K for **14** and at 378 K for **15**. Table 6 gives the results of the dynamic ^{13}C NMR studies of **14** and **15** and related compounds. The energy barriers $\Delta G_c^{\ddagger}$ for conformational inversions of **14** and **15** were found to be 14.4 and 19.4 kcal mol^{-1}, respectively. The *E*,*Z*-topomerizations of **14** and **15** were studied by ^{13}C NMR spectroscopy by monitoring the signals of the pair C^1 and C^8 in the selenoxanthenylidene and telluroxanthenylidene moieties in the temperature range 298–416 K (in Cl_2DC–$CDCl_2$). For this process, dynamic ^{13}C NMR is advantageous because the coalescence method can directly be applied to the first order ^{13}C spectra, while evaluation of the ^{1}H spectra would require line shape analysis, *i.e.*, simulation of the complicated spectra. The signals of C^1 and C^8 of **14** and **15** appeared in each compound as two singlets. No coalescence and no broadening of the C^1 and C^8 signals were observed up to 416 K. Table 6 summarizes the results of dynamic experiments

Table 7 Enthalpies of formation, conformational energies and strain energies of **7**–**10**, **12**, **13**, **35**, and **36**

	X, Y	Conformation[a]	Symmetry	[b]	ΔH_f°[c]	$\Delta\Delta H_f^{\circ}$[c]	SE[c,d]
10	Te, —	**au**	C_s	Min	147.235	0.0	6.2
10	Te, —	**t**	C_2	TS	168.857	21.6	27.8
10	Te, —	$\mathbf{t}_\perp$	C_{2v}	TS	181.202	34.0	40.1
9	Se, —	**au**	C_s	Min	123.920	0.0	8.2
9	Se, —	**t**	C_2	TS	138.709	14.8	23.0
9	Se, —	$\mathbf{t}_\perp$	C_{2v}	TS	150.902	27.0	35.2
13	S, —	**au**	C_s	Min	142.652	0.0	11.2
13	S, —	**t**	C_2	Min	153.659	11.0	22.2
13	S, —	$\mathbf{t}_\perp$	C_{2v}	TS	165.418	22.8	34.0
12	O, —	**au**	C_s	Min	104.117	0.0	15.4
12	O, —	**t**	C_2	Min	107.486	3.4	18.8
12	O, —	$\mathbf{t}_\perp$	C_{2v}	TS	123.763	19.6	35.1
8	Te, Te	**af**	C_{2h}	Min	158.113	0.0	3.7
8	Te, Te	**sf**	C_{2v}	Min	148.404	−9.7	−6.1
8	Te, Te	**t**	D_2	TS	195.648	37.5	41.2
8	Te, Te	$\mathbf{t}_\perp$	D_{2d}	3	196.988	38.9	42.5
7	Se, Se	**af**	C_{2h}	Min	108.814	0.0	5.1
7	Se, Se	**sf**	C_{2v}	Min	112.118	3.3	8.4
7	Se, Se	**t**	D_2	TS	135.061	26.2	31.3
7	Se, Se	$\mathbf{t}_\perp$	D_{2d}	TS	136.464	27.6	32.7
35	Se	**f**	C_s	Min	60.177	0.0	
35	Se	**p**	C_{2v}	TS	61.056	0.9	
36	Te	**f**	C_s	Min	85.546	0.0	
36	Te	**p**	C_{2v}	TS	91.610	6.1	

[a] Conformation: **au**: unevenly *anti*-folded; **t**: twisted; $\mathbf{t}_\perp$: orthogonally twisted; **af**: *anti*-folded; **sf**: *syn*-folded; **f**: folded; **p**: planar. [b] Minima (Min), transition states (TS), or number of imaginary frequencies for higher order saddle points. [c] In kcal mol^{-1}. [d] For a definition of the strain energies (SE) see ref. 3 and 19.

of the *E*,*Z*-topomerization. The energy barriers for *E*,*Z*-topomerization of **14** and **15** were found to be higher than 21.6 kcal mol^{-1}. The results of the DNMR experiments indicated that the barriers for conformational inversions of **11** increase in the series X = O, S, Se, Te. It is interesting to note that the fluorenylidene type bistricyclic enes have distinct barriers for conformational inversion and *E*,*Z*-isomerization. In homomerous bistricyclic enes with central six-membered rings identical barriers for *E*,*Z*-isomerization and conformational inversion were found.[4,16]

Semiempirical calculations

Recently, a systematic survey of overcrowded homomerous and heteromerous bistricyclic aromatic enes (**1**) has been carried out, using the semiempirical PM3 method.[3] Moreover, the dynamic stereochemistry of homomerous **1** has been studied using PM3 calculations.[4] The present article reports the results of PM3 calculations of the selenium- and tellurium-bridged heteromerous bistricyclic enes **9** and **10** and their comparison with the homomerous **7** and **8**. The following conformations have been calculated using the semiempirical PM3[41] method as implemented in MOPAC 6.00:[42] C_{2h} *anti*-folded (**af**), C_{2v} *syn*-folded (**sf**), D_2 twisted (**t**), and D_{2d} orthogonally twisted ($\mathbf{t}_\perp$) for the homomerous enes, and C_s *anti*-folded with uneven degrees of folding (**au**), C_2 twisted (**t**), and C_{2v} orthogonally twisted ($\mathbf{t}_\perp$) for the heteromerous fluorenylidenechalcoxanthenes. The orthogonally twisted conformations are biradicals. For the fluorenylidenechalcoxanthenes, *syn*-folded conformations could not be found; all starting structures converged to the *anti*-folded conformations **au**. For comparison, the C_{2v} planar (**p**) and C_s folded (**f**) conformations of the 9-methylidenechalcoxanthenes (**35** heteroatom = Se, **36** heteroatom = Te, and **37** heteroatom = S) were also calculated. The various conformations have been fully optimized and frequencies have been calculated. The *anti*-folded and *syn*-folded conformations of **7**–**10**, **12**, and **13** are *bona fide* minima. The twisted conformations of **12** and **13** are minima, while those of **7**–**10** are transition states. Table 7 gives the semiempirical PM3 heats of formation (ΔH_f°) of the conformations of **7**–**10**, **12**, **13**, **35**, and **36**, the conformational energies ($\Delta\Delta H_f^{\circ}$) relative to the corresponding global minimum and the strain energies (SE) derived from suitable isodesmic reactions used previously.[3] Selected geometrical parameters are given in Table 1.

Among the conformations of **9** and **10**, the most stable ones are the *anti*-folded conformations **au-9** and **au-10**. The geometries agree well with the X-ray structures. Overcrowding and folding of the fluorenylidene moiety are higher in **au-9** than in **au-10**. This strain is reflected in the higher strain energy SE(**au-9**) = 8.2 kcal mol^{-1}, as compared with SE(**au-10**) = 6.2 kcal mol^{-1}. The higher degree of folding in the telluroxanthenylidene moiety apparently costs little additional energy. Due to the longer bonds and smaller bond angle at Te, telluroxanthenylidene moieties are predetermined for high folding dihedrals as may be seen in 9-methylidenetelluroxanthene, which has no fjord region. The folding dihedral of **36** is 47.3°, while **35** is folded by 22.3°. Strain energy, fjord region overcrowding, and folding of the fluorenylidene moieties increase in the *anti*-folded conformations of the fluorenylidenechalcoxanthene series with decreasing size of the bridging atom Te, Se, S, O. The opposite trend is seen for the strain energies and conformational energies of the twisted conformations **t**. While PM3 calculates for **t-12** a conformational energy of only 3.4 kcal mol^{-1} and a subtle equilibrium between the folded and twisted conformations of fluorenylidenexanthenes has been noted, the twisted conformations of fluorenylidenethioxanthene, -selenoxanthene and -telluroxanthene have high conformational energies $\Delta\Delta H_f^{\circ}$(**t-13**) = 11.0 kcal mol^{-1}, $\Delta\Delta H_f^{\circ}$(**t-9**) = 14.8 kcal mol^{-1}, and $\Delta\Delta H_f^{\circ}$(**t-10**) = 21.6 kcal mol^{-1}. These twisted conformations have similar ethylenic twist angles of 41.4 to 43.7°. They are probably determined by the shortest acceptable nonbonding distances across the fjord regions: $C^1 \cdots C^{1'}$ = 298 (**t-10**) to 304 pm (**t-12**) (13 to 11% penetration), $C^1 \cdots H^{1'}$ = 259 (**t-10**) to 257 pm (**t-12**) (10% penetration), $H^1 \cdots C^{1'}$ = 268 (**t-10**) to 250 pm (**t-12**) (6% to 13% penetration), and $H^1 \cdots H^{1'}$ = 272 (**t-10**) to 243 pm (**t-12**) (5 to 15% penetration). In view of the similar degrees of twisting and overcrowding in the twisted conformations, the differences in strain energy SE are surprising. However, one should keep in mind the nearly planar chalcoxanthenylidene moieties of the twisted

Table 8 Crystallographic data for **9** and **10**

	9	**10**
Space group	$P2_1/c$	C_2
Crystal system	Monoclinic	Monoclinic
a/pm	1877.2(3)	1909.4(3)
b/pm	970.8(3)	556.1(1)
c/pm	2164.3(4)	1782.9(3)
β/deg	111.87	91.19(1)
V/pm^3	3660×10^6	1892.7×10^6(6)
Z	4	4
Asymmetric unit	$2 \times C_{26}H_{16}Se$	$C_{26}H_{16}Te$
ρ_{calc}/g cm^{-3}	1.48	1.68
$\mu(K_\alpha)$/cm^{-1}	28.55	15.80
Diffractometer	ENRAF-NONIUS CAD4	Philips PW1100/20
Radiation λ/pm	154.178	71.069
$2\theta_{max}$/deg	140	55
No. of unique reflections	7370	2399
No. of reflections with $I > 3\sigma_I$	6224	2005
R	0.034	0.044
R_w	0.058	0.056

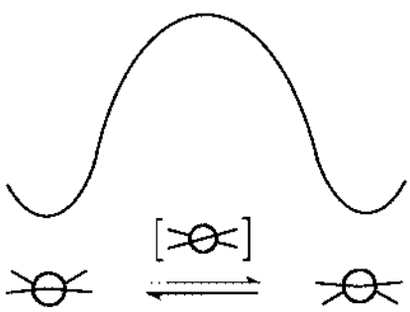

Fig. 4 Schematic mechanism for inversion of **au-9** and **au-10**.

conformations. Flattening the central rings takes increasing energy for X = S, Se, and Te. Thus: SE(**t-10**) − $\Delta\Delta H_f^o$(**p-36**) = 27.8 − 6.1 = 21.7 kcal mol^{-1}, SE(**t-9**) − $\Delta\Delta H_f^o$(**p-35**) = 23.0–0.9 = 22.1 kcal mol^{-1}, and SE(**t-13**) − $\Delta\Delta H_f^o$(**p-37**)[3] = 22.2 − 0.4 = 21.8 kcal mol^{-1}. In **9** and **10**, the twisted conformations **t-9** and **t-10** may serve as transition states for the inversion of **au-9** and **au-10**, respectively. The conformational energies $\Delta\Delta H_f^o$(**t-9**) = 14.8 kcal mol^{-1}, and $\Delta\Delta H_f^o$(**t-10**) = 21.6 kcal mol^{-1}, are in good agreement with the DNMR results, 14.4 and 19.4 kcal mol^{-1}, respectively. In **13**, the twisted conformation may be an intermediate in the inversion of **au-13** with a two-step mechanism similar to the inversion of **12**. The proposed mechanism of the conformational inversion of **au-9** and **au-10** is shown in Fig. 4.

The orthogonally twisted conformations of the fluorenylidenechalcoxanthenes are the transition states for *E*,*Z*-isomerization. The PM3 calculated conformational energy may serve to help prediction of the thermal *E*,*Z*-isomerization barrier. Thus the *E*,*Z*-isomerization barriers are 34.0 kcal mol^{-1} in **10**, 27.0 kcal mol^{-1} in **9**, 22.8 kcal mol^{-1} in **13**, and 19.6 kcal mol^{-1} in **12** (PM3). In **12**, the experimental barrier for *E*,*Z*-isomerization is 19.6 kcal mol^{-1}.[20] The orthogonally twisted conformations have planar tricyclic moieties and are not overcrowded.

In conclusion, in the fluorenylidenechalcoxanthenes (**11**), the chalcoxanthenylidene moiety determines the outcome of the competition between the twisted conformation and the folded conformation, in the solid state and in solution. The molecules of **9** and **10** adopt *anti*-folded and folded conformations, respectively, with 56.3 and 62.0°, and 10.2 and 8.0° (**9a** and **9b**) and 63.6 and 2.2° (**10**) folding dihedrals. The DNMR conformational inversion barriers of the isopropyl derivatives **14** and **15** are in good agreement with the PM3 results. The *E*,*Z*-isomerization barriers were too high for the DNMR method. Distinct barriers for conformational inversion and for *E*,*Z*-isomerization were found in the fluorenylidene-selenoxanthene and -telluroxanthene. Conformational inversions of **9** and **10** proceed *via* the twisted transition state corresponding to calculated barriers of 14.8 and 21.6 kcal mol^{-1}, in excellent agreement with experiment. The *E*,*Z*-isomerizations proceed *via* orthogonally twisted biradical transition states with predicted barriers of 27.0 (**9**) and 34.0 kcal mol^{-1} (**10**) (PM3). In the fluorenylidenechalcoxanthenes, the 5-ring bond angles open up the fjord regions and facilitate an edge-passage[4] in the conformational inversion. This effect lowers the transition states for the conformational inversion to below the orthogonally twisted transition states for the *E*,*Z*-isomerization.

Experimental

Melting points are uncorrected. All NMR spectra were recorded with a Bruker DRX 400 spectrometer; ^{1}H NMR spectra were recorded at 400.1 MHz using $CDCl_3$ as solvent and as internal standard ($\delta(CHCl_3)$ = 7.26 ppm). ^{13}C NMR spectra were recorded at 100.6 MHz using $CDCl_3$ as solvent and as internal standard ($\delta(CDCl_3)$ = 77.01 ppm). ^{77}Se NMR spectra were recorded at 76.3 MHz using $CDCl_3$ as a solvent and selenoxanthone (**20**) as external standard δ = 334.7 ppm (relative to Me_2Se in $CDCl_3$).[43] ^{125}Te NMR spectra were recorded at 126.2 MHz using $CDCl_3$ as solvent and telluroxanthone (**21**) as external standard δ = 473.6 ppm (relative to Me_2Te in C_6D_6, in DMSO-d_6, δ(**21**) = 471.5 ppm).[43] Bistricyclic aromatic enes (**1**) and their precursors give rise to ABCD type ^{1}H NMR spectra. In many cases, these spectra are sufficiently resolved at 400 MHz to be interpreted in terms of first-order multiplets and the coupling constants J of the doublet splittings could be determined. Hydrogens H^1, H^4, H^5, and H^8 have one *ortho* coupling constant (^3J = 6.2–8.8 Hz), one *meta* coupling constant (^4J = 1.0–1.8 Hz) and one *para* coupling constant (^5J = 0.4–0.8 Hz). These multiplets appear as doublet of doublet of doublets (ddd). In the case of hydrogens H^2, H^3, H^6, and H^7 there are two *ortho* coupling constants (^3J) and one *meta* coupling constant (^4J). Since the two major coupling constants are similar, these multiplets look like a triplet of doublets (td) (or triplet in case ^4J is not resolved). Whenever two ^3J could be determined, the individual values are reported. Multiplicity h indicates a heptet. UV/VIS spectra were measured using a UVIKON 860 spectrometer. IR spectra were measured with a Perkin Elmer System 2000 FT-IR spectrometer.

Elemental microanalyses were determined by Chemisar Laboratories Inc., N. Guelph, Ontario, Canada. Single crystals were obtained by slow sublimation in a high vacuum sealed tube at 200–250 °C in a Büchi GKR 50 oven.

X-Ray crystallographic analysis ‡

The crystal data of **9** and **10** are given in Table 8. The lattice parameters were obtained by a least-squares fit of 24 centered reflections. Intensity data were collected using the ω–2θ technique. The scan width, $\Delta\omega$, for each reflection was 1.00 + 0.35tan θ for Mo radiation and 0.80 + 0.15tan θ for Cu radiation. The intensities of three standard reflections were monitored during data collection, and no decay was observed. Intensities were corrected for Lorentz and polarization effects. The positions of all non-hydrogen atoms were obtained using the results of the SHELXS-86 direct method analysis.[44] After several cycles of refinements the positions of the hydrogen atoms were either found, for compound **9** or calculated for **10**, and added to the refinement process. All non-hydrogen atoms were refined anisotropically, while the positions of hydrogen atoms were refined isotropically for **9** or kept fixed, using a riding model for compound **10**. The refinement proceeded to convergence by minimizing the function $\Sigma w(|F_o| - |F_c|)^2$ with $w = \sigma_F^{-2}$.

Synthesis

9-Diazo-9*H*-fluorene (24). Diazo derivative **24** was prepared according to the literature.[31] Mp 95 °C (lit.[31] mp 94–95 °C). ^{1}H NMR ($CDCl_3$): δ 7.360 (td, ^3J = 7.5 Hz, ^4J = 1.2 Hz, 2H, H^3, H^6), 7.420 (td, ^3J = 7.4 Hz, ^4J = 1.2 Hz, 2H, H^2, H^7), 7.530 (ddd, ^3J = 7.7 Hz, ^4J = 1.2 Hz, ^5J = 0.8 Hz, 2H, H^1, H^8), 7.970 (ddd, ^3J = 7.6 Hz, ^4J = 1.2 Hz, ^5J = 0.8 Hz, 2H, H^4, H^5). ^{13}C NMR ($CDCl_3$): δ 63.37 (C=N), 119.27 (C-H), 120.92 (C-H), 124.48 (C-H), 126.28 (C-H), 131.41 (C), 132.94 (C).

Dispiro[9*H*-fluorene-9,2′-thiirane-3′,9″-(9″*H*-selenoxanthene)] (25). To a stirred solution of thioketone **22**[19] (0.250 g, 0.909 mmol) in anhydrous benzene (40 mL) protected by a $CaCl_2$ tube, diazo derivative **24** (0.183 g, 0.954 mmol) was added. The dark color slowly disappeared, while the reaction mixture was refluxed for 4 h. The termination of the reaction was determined by NMR. The solution was evaporated under reduced pressure. The crude product was triturated and the precipitate was filtered off. A light yellow powder was obtained, 0.333 g, 83% yield; mp 218 °C. ^{1}H NMR ($CDCl_3$): δ 6.326 (d, ^3J = 7.7 Hz, 2H), 6.768 (t, ^3J = 7.5 Hz, 2H), 7.129 (td, ^3J = 7.5 Hz, ^4J = 1.1 Hz, 2H), 7.183 (t, ^3J = 7.6 Hz, 2H), 7.357–7.407 (m, 4H), 7.602 (d, ^3J = 7.5 Hz, 2H), 8.021 (ddd, ^3J = 7.7 Hz, ^4J = 1.5 Hz, ^5J = 0.8 Hz, 2H). ^{13}C NMR ($CDCl_3$): δ 58.02 (C-S), 64.35 (C-S), 119.55 (C-H), 123.68 (C-H), 126.06 (C-H), 126.44 (C-H), 126.93 (C), 127.76 (C), 129.95 (C-H), 130.10 (C-H), 135.33 (C), 138.85 (C), 141.14 (C-H), 142.87 (C-H). ^{77}Se NMR ($CDCl_3$): δ 390.13.

9-(9′*H*-Fluoren-9′-ylidene)-9*H*-selenoxanthene (9). To a stirred solution of dispirothiirane **25** (0.150 g, 0.341 mmol) in anhydrous benzene (30 mL), protected by a $CaCl_2$ tube, PPh_3 (0.093 g, 0.358 mmol) was added. After refluxing for 12 h, the mixture was cooled to rt, and the solvent was removed under reduced pressure. Trituration of the crude product in boiling ethanol gave a precipitate, which was filtered off. A light yellow powder was obtained, 0.069 g, yield 50%; mp 230–232 °C. A sample for analysis was purified by column chromatography on dry silica gel using petrol ether–Et_2O 96 : 4 as eluent. ^{1}H NMR ($CDCl_3$): δ 6.946 (td, ^3J = 8.0 Hz, ^3J = 7.4 Hz, ^4J = 1.2, 2H, H$^{2'}$, H$^{7'}$), 7.129 (ddd, ^3J = 8.0 Hz, ^4J = 1.7 Hz, ^5J = 0.8 Hz, 2H, H$^{1'}$, H$^{8'}$), 7.237–7.281 (m, 4H, H$^{3'}$, H$^{6'}$, H^2, H^7), 7.330 (td, ^3J = 7.5 Hz, ^4J = 1.3 Hz, 2H, H^3, H^6), 7.659 (ddd, ^3J = 7.5 Hz, ^4J = 1.2 Hz, ^5J = 0.7 Hz, 2H, H$^{4'}$, H$^{5'}$), 7.778 (ddd, ^3J = 7.5 Hz, ^4J = 1.5 Hz, ^5J = 0.4 Hz, 2H, H^1, H^8), 7.823 (ddd, ^3J = 7.6 Hz, ^4J = 1.3 Hz, ^5J = 0.5 Hz, 2H, H^4, H^5). ^{13}C NMR ($CDCl_3$): δ 119.33 (C$^{4'}$, C$^{5'}$), 125.59 (C$^{1'}$, C$^{8'}$), 126.22 (C$^{2'}$, C$^{7'}$), 126.60 (C^3, C^6), 127.25 (C^2, C^7), 128.30 (C$^{3'}$, C$^{6'}$), 129.30 (C^1, C^8), 131.23 (C^4, C^5), 131.55 (C$^{9'}$), 133.35 (C^{4a}, C^{10a}), 137.99 (C$^{8a'}$, C$^{9a'}$), 138.61 (C^{8a}, C^{9a}), 140.33 (C^9), 140.94 (C$^{4a'}$, C$^{4b'}$). ^{77}Se NMR ($CDCl_3$): δ 398.20. UV/VIS (cyclohexane): $c = 3.87 \times 10^{-5}$ M, λ_{max}/nm (ε/M^{-1} cm^{-1}): 331 (18101).Calc. for $C_{26}H_{16}Se$: C, 76.66; H, 3.93; Se, 19.38. Found: C, 76.36; H, 3.94; Se, 19.05%. MS, *m*/*z* (% molecular ion): 409.04462 (5%, $^{12}C_{25}{}^{13}CH_{16}{}^{80}Se$), 408.04140 (19%, $^{12}C_{26}H_{16}{}^{80}Se$, and/or $^{12}C_{25}{}^{13}CH_{15}{}^{80}Se$), 406.04256 (7%, $^{12}C_{26}H_{16}{}^{78}Se$, $^{12}C_{25}{}^{13}CH_{15}{}^{78}Se$).

Dispiro[9*H*-fluorene-9,2′-thiirane-3′,9″-(9″*H*-telluroxanthene)] (26). Dispirothiirane **26** was obtained analogously to dispirothiirane **25** with some modifications. To a stirred solution of thioketone **23**[19] [freshly prepared from ketone **21** (0.307 g, 1.000 mmol), Lawesson's reagent (2,4-bis(4-methoxyphenyl)-1,3,2λ^5,4λ^5-dithiadiphosphetane-2,4-dithione), 0.202 g, 0.500 mmol, in dried benzene (30 mL)] in anhydrous benzene (30 mL) protected by a $CaCl_2$ tube, diazo derivative **24** (0.211 g, 1.090 mmol) was added. The reaction mixture was refluxed for 6 h. Work-up as in the procedure of **25** gave light orange powder, 0.311 g of **26**, in 64% yield; mp 168–172 °C. ^{1}H NMR ($CDCl_3$): δ 6.167 (ddd, ^3J = 7.8 Hz, ^4J = 1.0 Hz, ^5J = 0.7 Hz, 2H), 6.767 (td, ^3J = 7.8 Hz, ^3J = 7.5 Hz, ^4J = 1.1 Hz, 2H), 7.069 (td, ^3J = 7.5 Hz, ^4J = 1.4 Hz, 2H), 7.186 (td, ^3J = 7.5 Hz, ^4J = 1.1 Hz, 2H), 7.382 (td, ^3J = 7.7 Hz, ^3J = 7.4 Hz, ^4J = 1.3 Hz, 2H), 7.585 (ddd, ^3J = 7.5 Hz, ^4J = 1.2 Hz, ^5J = 0.4 Hz, 2H), 7.618 (ddd, ^3J = 7.6 Hz, ^4J = 1.2 Hz, ^5J = 0.7 Hz, 2H), 8.048 (ddd, ^3J = 7.7 Hz, ^4J = 1.4 Hz, ^5J = 0.4 Hz, 2H). ^{13}C NMR ($CDCl_3$): δ 58.49 (C-S), 69.34 (C-S), 119.55 (C-H), 122.36 (C), 123.78 (C-H), 126.08 (C-H), 126.89 (C-H), 127.19 (C-H), 127.73 (C-H), 131.05 (C-H), 135.82 (C-H), 141.33 (C), 141.77 (C), 143.30 (C). ^{125}Te NMR ($CDCl_3$): δ 613.47.

9-(9′*H*-Fluoren-9′-ylidene)-9*H*-telluroxanthene (10). Compound **10** was obtained analogously to **9**. A solution of dispirothiirane **26** (0.170 g, 0.348 mmol), and PPh_3 (0.081 g, 0.310 mmol), in anhydrous benzene (30 mL) protected by a $CaCl_2$ tube, was refluxed for 4 h. Trituration of the crude material in hot ethanol gave **10**, 0.086 g, yield 76%; mp 252–254 °C. A sample for analysis was purified by column chromatography on dry silica gel using petrol ether–Et_2O (96 : 4) as eluent. ^{1}H NMR ($CDCl_3$): δ 6.878–6.929 (m, 4H, H$^{1'}$, H$^{8'}$, H$^{2'}$, H$^{7'}$), 7.179 (td, ^3J = 7.5 Hz, ^4J = 1.4 Hz, 2H, H^3, H^6), 7.229 (m, 2H, H$^{3'}$, H$^{6'}$), 7.344 (td, ^3J = 7.5 Hz, ^4J = 1.3 Hz, 2H, H^2, H^7), 7.658 (dd, ^3J = 7.6 Hz, ^4J = 1.0 Hz, 2H, H$^{4'}$, H$^{5'}$), 7.733 (ddd, ^3J = 7.7 Hz, ^4J = 1.5 Hz, ^5J = 0.5 Hz, 2H, H^1, H^8), 8.004 (ddd, ^3J = 7.7 Hz, ^4J = 1.2 Hz, ^5J = 0.5 Hz, 2H, H^4, H^5). ^{13}C NMR ($CDCl_3$): δ 118.94 (C^{4a}, C^{10a}), 119.31 (C$^{4'}$, C$^{5'}$), 125.65 (C$^{1'}$, C$^{8'}$), 126.36 (C$^{2'}$, C$^{7'}$), 127.16 (C^3, C^6), 127.57 (C^2, C^7), 128.26 (C$^{3'}$, C$^{6'}$), 129.10 (C^1, C^8), 131.37 (C$^{9'}$), 136.99 (C^4, C^5), 137.96 (C$^{8a'}$, C$^{9a'}$), 140.90 (C$^{4a'}$, C$^{4b'}$), 142.39 (C^{8a}, C^{9a}), 145.75 (C^9). ^{125}Te NMR ($CDCl_3$): δ 620.93. UV/VIS (cyclohexane): $c = 1.64 \times 10^{-4}$ M, λ_{max}/nm (ε/M^{-1} cm^{-1}): 327 (17796). Calc. for $C_{26}H_{16}Te$: C, 68.48; H, 3.53; Te, 27.98. Found: C, 68.29; H, 3.57; Te, 27.84%. MS, *m*/*z* (% molecular ion): 459.03713 (20%, $^{12}C_{25}{}^{13}CH_{16}{}^{130}Te$), 458.03319 (70%, $^{12}C_{26}H_{16}{}^{130}Te$), 457.03460 (19%, $^{12}C_{25}{}^{13}CH_{16}{}^{128}Te$), 455.03240 (13%, $^{12}C_{25}{}^{13}CH_{16}{}^{126}Te$), 454.03016 (41%, $^{12}C_{26}H_{16}{}^{126}Te$, and/or $^{12}C_{25}{}^{13}CH_{16}{}^{126}Te$), 453.02972 (16%, $^{12}C_{26}H_{16}{}^{125}Te$), 327.11671 (100%, $^{12}C_{26}H_{15}$).

9-Diazo-2-(1′-methylethyl)-9*H*-fluorene (27). Prepared according to the literature.[32] A red powder, 0.791 g, yield 88%; mp 66 °C. ^{1}H NMR ($CDCl_3$): δ 1.334 (CH(C*H*$_3$)$_2$), 6H), 3.041 (C*H*(CH$_3$)$_2$, 1H), 7.200 (ddd, 1H), 7.294–7.370 (m, 3H), 7.486 (ddd, 1H), 7.855 (d, 1H), 7.896 (ddd, 1H). ^{13}C NMR ($CDCl_3$): δ 24.24 (CH(*C*H$_3$)$_2$), 34.48 (*C*H(CH$_3$)$_2$), 117.06 (C-H), 119.28 (C-H), 119.81 (C), 120.65 (C-H), 120.84 (C-H), 123.50 (C-H), 124.48 (C-H), 125.84 (C-H), 127.38 (C), 129.01 (C), 147.68 (C).

‡ CCDC reference numbers 164943 and 164944. See http://www.rsc.org/suppdata/p2/b1/b104858a/ for crystallographic files in .cif or other electronic format.

2-(1‴-Methylethyl)dispiro[9*H*-fluorene-9,2′-thiirane-3′,9″-(9″*H*-selenoxanthene)] (28). To a stirred solution of diazo derivative **27** (0.223 g, 0.954 mmol) in anhydrous benzene (30 mL), protected by a $CaCl_2$ tube, thioketone **22** (0.250 g, 0.909 mmol) was added. The reaction mixture was refluxed for 8 h to give a mixture which was dark green. The termination of the reaction was determined by NMR. The solvent was evaporated under reduced pressure. The ^{77}Se NMR spectrum of the crude product gave the following signals: 362.9 ppm selenoxanthione (**22**), 364.6 ppm dispiro[9*H*-selenoxanthene-9,2′-thiirane-3′,9″-(9″*H*-selenoxanthene)], and 391.1 ppm (**28**). The crude product was dissolved in CH_2Cl_2 and chromatographed on a dry silica gel column using a petrol ether–CH_2Cl_2 gradient (2 to 10%). The desired dispirothiirane was isolated as a yellow oil (0.200 g, 45%), with some impurities (^{77}Se NMR, 364.6) and a new signal that probably indicated a sulfur elimination that occurred on the column yielding the ethylene **14**. ^{1}H NMR ($CDCl_3$): δ 0.933 (d, 3H), 1.006 (d, 3H), 2.630 (h, 1H), 6.286 (d, 1H), 6.362 (dd, 1H), 6.773 (td, 1H), 7.062 (d, 1H), 7.161 (m, 3H), 7.382–7.450 (m, 4H), 7.485 (dd, 1H), 7.584 (dd, 1H), 8.070 (m, 2H). ^{13}C NMR ($CDCl_3$): δ 23.57, 24.15, 34.04 [CH(CH_3)$_2$], 57.95 (C-S), 64.30 (C-S), 119.23 (C-H), 121.66 (C-H), 123.64 (C-H), 125.55 (C-H), 126.38 (C-H), 126.45 (C-H), 126.79 (C), 126.86 (C-H), 126.89 (C-H), 127.68 (C-H), 128.35 (C), 129.93 (C-H), 130.01 (C-H), 130.04 (C-H), 131.78 (C), 135.32 (C), 135.48 (C), 138.87 (C-H), 138.90 (C-H), 141.33 (C), 142.85 (C), 142.87 (C), 147.11 (C-H). ^{77}Se NMR ($CDCl_3$): δ 391.13.

9-(2′-(1″-Methylethyl)-9′*H*-fluoren-9′-ylidene)-9*H*-selenoxanthene (14). To a stirred solution of dispirothiirane **28** (0.100 g, 0.208 mmol) in anhydrous benzene (30 mL), protected by a $CaCl_2$ tube, PPh_3 (0.060 g, 0.228 mmol) was added. After refluxing for 7 h, the mixture was cooled to rt, and the solvent was removed under reduced pressure. Trituration of the crude product in hot ethanol gave a yellow powder (0.057 g). It was dissolved in CH_2Cl_2, and chromatographed on a dry silica gel column using petrol ether–Et_2O 98 : 2 as eluent. Thus, **14** was obtained as a yellow powder (0.045 g), yield 48%. ^{1}H NMR ($CDCl_3$): δ 1.086 (br s, 6H, CH(CH_3)$_2$), 2.713 (h, J = 6.9 Hz, 1H, C*H*(CH_3)$_2$), 6.926 (td, ^3J = 8.0 Hz, ^3J = 7.3 Hz, ^4J = 1.4 Hz, 1H, H$^{7'}$), 7.078 (d, 1H, H$^{1'}$), 7.122 (ddd, ^3J = 7.8 Hz, ^4J = 1.6 Hz, ^5J = 0.4 Hz, 1H, H$^{3'}$), 7.188 (dd, ^3J = 7.2 Hz, ^5J = 0.5 Hz, 1H, H$^{8'}$), 7.237 (td, ^3J = 7.5 Hz, ^4J = 1.0 Hz, 1H, H$^{6'}$), 7.262–7.300 (m, 2H, H^2, H^7), 7.319–7.363 (m, 2H, H^3, H^6), 7.565 (d, J = 7.7 Hz, 1H, H$^{4'}$), 7.621 (ddd, ^3J = 7.6 Hz, ^4J = 1.1 Hz, ^5J = 0.7 Hz, 1H, H$^{5'}$), 7.780–7.860 (m, 4H, H^1, H^8, H^4, H^5). ^{13}C NMR ($CDCl_3$): δ 23.86 (CH(CH_3)$_2$), 34.17 (CH(CH_3)$_2$), 119.03 (C$^{5'}$), 119.07 (C$^{4'}$), 123.70 (C$^{1'}$), 125.52 (C$^{8'}$), 125.73 (C$^{7'}$), 126.45 (C^3 or C^6), 126.58 (C^6 or C^3), 127.07 (C^2, or C^7, or C$^{3'}$), 127.14 (C^7, or C^2, or C$^{3'}$), 127.19 (C$^{3'}$, or C^2, or C^7), 128.26 (C$^{6'}$), 129.31 (C^1, or C^8), 129.48 (C^8, or C^1), 131.17 (C^4, or C^5), 131.21 (C^5, or C^4), 131.78 (C), 133.39 (C), 133.44 (C), 138.09 (C), 138.31 (C), 138.62 (C), 138.65 (C), 138.81 (C), 139.79 (C), 141.12 (C), 147.02 (C). ^{77}Se NMR ($CDCl_3$): δ 397.74.

2-(1‴-Methylethyl)dispiro[9*H*-fluorene-9,2′-thiirane-3′,9″-(9″*H*-telluroxanthene)] (29). Dispirothiirane **29** was obtained analogously to dispirothiirane **28** with some modifications. To a stirred solution of thioketone **23** [freshly prepared from ketone **21** (0.350 g, 1.130 mmol), Lawesson's reagent (0.223 g, 0.568 mmol), in dried benzene (40 mL)] in anhydrous benzene (40 mL) and protected by a $CaCl_2$ tube, diazo derivative **27** (0.309 g, 1.320 mmol) was added. The reaction mixture was refluxed for 0.5 h and the color of the reaction mixture became light. Trituration of the crude product in boiling ethanol gave 0.315 g of **29** with 10% of impurities. ^{1}H NMR ($CDCl_3$): δ 0.868 (d, 3H, CH(CH_3)$_2$), 0.942 (d, 3H, CH(CH_3)$_2$), 2.568 (h, 1H, C*H*(CH_3)$_2$), 6.089 (d, 1H), 6.154 (d, 1H), 6.727 (td, 1H), 7.021–7.082 (m, 3H), 7.159 (td, 1H), 7.359–7.419 (m, 2H), 7.507 (d, 1H), 7.557–7.586 (m, 3H), 8.061 (td, 2H). ^{13}C NMR ($CDCl_3$): δ 23.45 (CH(CH_3)$_2$), 24.14 (CH(CH_3)$_2$), 34.01 (*C*H(CH_3)$_2$), 58.39 (C-S), 69.26 (C-S), 119.18 (C-H), 119.23 (C-H), 121.79 (C-H), 122.37 (C), 122.52 (C), 123.73 (C-H), 125.56 (C-H), 126.43 (C-H), 126.84 (C-H), 126.89 (C-H), 127.10 (C-H), 127.15 (C-H), 127.65 (C-H), 131.05 (C-H), 131.13 (C-H), 135.70 (C-H), 135.75 (C-H), 136.00 (C), 139.08 (C), 139.98 (C), 141.53 (C), 141.79 (C), 143.27 (C), 147.09 (C). ^{125}Te NMR ($CDCl_3$): δ 615.63.

9-(2′-(1″-methylethyl)-9′*H*-fluoren-9′-ylidene)-9*H*-telluroxanthene (15). Compound **15** was obtained analogously to **14**. A solution of **29** (0.150 g, 0.283 mmol), and PPh_3 (0.089 g, 0.339 mmol), in anhydrous benzene (30 mL) protected by a $CaCl_2$ tube, was refluxed for 5 h. Trituration of the crude material in hot ethanol gave **15**, 0.113 g in 80% yield. Further purification was done by chromatography on a dry silica gel column with petrol ether–ether 98 : 2 as an eluent; even after the column 10% of the homomerous **8** was detected. ^{1}H NMR ($CDCl_3$): δ 1.017 (d, J = 6.9 Hz, 3H, CH(CH_3)$_2$), 1.081 (d, J = 6.9 Hz, 3H, CH(CH_3)$_2$), 2.680 (h, J = 6.9 Hz, 1H, C*H*(CH_3)$_2$), 6.807 (d, 1H, H$^{1'}$), 6.894– 6.938 (m, 2H, H$^{7'}$, H$^{8'}$), 7.107 (ddd, ^3J = 7.8 Hz, ^4J = 1.6 Hz, ^5J = 0.5 Hz, 1H, H$^{3'}$), 7.176–7.244 (m, 3H, H^3, H^6, H$^{6'}$), 7.323–7.376 (m, 2H, H^2, H^7), 7.558 (dd, ^3J = 7.8 Hz, ^5J = 0.4 Hz, 1H, H$^{4'}$), 7.611 (d, ^3J = 7.5 Hz, 1H, H$^{5'}$), 7.726–7.763 (m, 2H, H$^{1'}$, H$^{8'}$), 7.992–8.031 (m, 2H, H^4, H^5). ^{13}C NMR ($CDCl_3$): δ 23.69 (CH(CH_3)$_2$), 23.96 (CH(CH_3)$_2$), 34.12 (*C*H(CH_3)$_2$), 119.00 (C$^{5'}$, or C$^{4'}$), 119.04 (C$^{4'}$, or C$^{5'}$), 123.79 (C$^{1'}$), 125.56 (C$^{7'}$, or C$^{8'}$), 125.85 (C$^{8'}$, or C$^{7'}$), 127.00 (C^3, or C^6), 127.04 (C^6, or C^3), 127.11 (C$^{3'}$), 127.43 (C^2, or C^7), 127.53 (C^7, or C^2), 128.20 (C$^{6'}$), 129.11 (C^1, or C^8), 129.27 (C^8, or C^1), 131.60 (C), 136.90 (C^4, or C^5), 136.93 (C^5, or C^4), 138.05 (C), 138.26 (C), 138.75 (C), 141.07 (C), 142.38 (C), 142.42 (C), 145.22 (C), 147.12 (C). ^{125}Te NMR ($CDCl_3$): δ 619.17.

11*H*-Benzo[*b*]fluoren-11-one. Prepared according to the literature,[35] yield 35%; mp 152–154 °C (lit.[35] mp 152 °C). ^{1}H NMR ($CDCl_3$): δ 7.370 (td, ^3J = 7.5 Hz, ^4J = 1.0 Hz, 1H), 7.480 (td, ^3J = 8.1 Hz, ^3J = 6.9 Hz, ^4J = 1.2 Hz, 1H), 7.550–7.600 (m, 2H), 7.740 (ddd, ^3J = 7.5 Hz, ^4J = 1.5 Hz, ^5J = 0.8 Hz, 1H), 7.780 (ddd, ^3J = 7.5 Hz, ^4J = 1.2 Hz, ^5J = 0.5 Hz, 1H), 7.860 (ddd, ^3J = 8.6 Hz, ^4J = 1.2 Hz, ^5J = 0.5 Hz, 1H), 7.890 (s, 1H, H^5), 7.910 (ddd, ^3J = 8.6 Hz, ^4J = 1.3 Hz, ^5J = 0.8 Hz, 1H), 8.200 (s, 1H, H^{10}). ^{13}C NMR ($CDCl_3$): δ 119.09 (C-H), 121.01 (C-H), 124.50 (C-H), 125.73 (C-H), 126.95 (C-H), 128.78 (C-H), 129.02 (C-H), 129.21 (C-H), 130.84 (C-H), 132.82 (C), 133.66 (C), 135.04 (C-H), 136.20 (C), 136.94 (C), 138.43 (C), 144.87 (C), 193.15 (C=O).

11-Diazo-11*H*-benzo[*b*]fluorene (30). *(i) Preparation of 11H-benzo[b]fluoren-11-one hydrazone.* To a stirred solution of 11*H*-benzo[*b*]fluoren-11-one (1.500 g, 6.46 mmol) in ethanol (60 mL), hydrazine hydrate (1.60 mL, 33 mmol) was added. The yellow reaction mixture turned orange and was refluxed for 9 h. During the reflux crystals were obtained, the mixture was cooled to rt and the crystals were filtered. Orange crystals of the hydrazone were obtained (1.426 g), yield 90%; the ratio between the two isomers was 1 : 0.65; mp 186–188 °C; TLC toluene–chloroform 8 : 2, R_f = 0.23. ^{1}H NMR ($CDCl_3$): major isomer, δ 6.455 (br s, N-H), 7.386 (td), 7.423 (td), 7.468 (td), 7.490–7.590 (m), 7.810 (ddd), 7.919 (ddd), 8.143 (s), 8.421 (s); minor isomer, δ 6.424 (br s, N-H), 7.432 (td), 7.490–7.590 (m), 7.890 (ddd), 7.960 (ddd), 8.204 (ddd), 8.084 (s), 8.201 (s).

*(ii) 11-Diazo-11H-benzo[b]fluorene (**30**).* Mercury oxide (2.46 g, 11.3 mmol), anhydrous sodium sulfate (0.62 g) and 11*H*-benzo[*b*]fluoren-11-one hydrazone (1.40 g, 5.69 mmol) were ground together for a few minutes, then transferred to a dry flask equipped with a magnetic stirrer protected by a $CaCl_2$ tube and dry Et_2O (30 mL) added. After a few minutes, a freshly

prepared, concentrated solution of KOH in ethanol was added (2.5 mL). The color of the solution changed gradually from orange to wine-red. The reaction was stirred at rt for 5 h. The progress of the reaction was monitored by TLC on silica gel (toluene–chloroform 8 : 2, $R_f = 0.92$). The solution was filtered and the residue was washed with Et_2O. The combined organic fractions were evaporated under reduced pressure, to give **30** as red crystals, 1.203 g, yield 87%; mp 134–136 °C (lit.[45] mp 138 °C). ^{1}H NMR ($CDCl_3$): δ 7.370 (td, $^3J = 7.1$ Hz, $^3J = 6.2$ Hz, $^4J = 1.4$ Hz, 1H), 7.450 (td, $^3J = 7.0$ Hz, $^4J = 1.1$ Hz, 1H), 7.478–7.518 (m, 3H), 7.861 (s, 1H, H^5), 7.889 (ddd, $^3J = 8.8$ Hz, $^4J = 1.3$ Hz, $^5J = 0.6$ Hz, 1H), 7.968 (ddd, $^3J = 8.2$ Hz, $^4J = 1.5$ Hz, $^5J = 0.5$ Hz, 1H), 8.059 (ddd, $^3J = 8.6$ Hz, $^4J = 1.1$ Hz, $^5J = 0.8$ Hz, 1H), 8.380 (s, 1H, H^{10}). ^{13}C NMR ($CDCl_3$): δ 63.44 (C=N_2), 117.20 (C-H), 119.40 (C-H), 119.61 (C-H), 121.39 (C-H), 124.78 (C-H), 124.93 (C-H), 125.88 (C-H), 127.11 (C-H), 127.60 (C-H), 128.54 (C-H), 131.25 (C), 131.39 (C), 131.59 (C), 131.69 (C), 132.59 (C), 133.63 (C). IR, Nujol λ_{max}/cm^{-1}: 2064, 1717, 878, 738.

Dispiro[11*H*-benzo[*b*]fluorene-11,2′-thiirane-3′,9″-(9″*H*-selenoxanthene)] (32). To a stirred solution of diazo derivative **30** (0.186 g, 0.763 mmol) in anhydrous benzene (30 mL) protected by a $CaCl_2$ tube, thioketone **22** (0.212 g, 0.772 mmol) was added. The dark color slowly became wine-red, while the reaction mixture was refluxed for 7 h. The termination of the reaction was determined by NMR. The solvent was evaporated under reduced pressure. The crude product was triturated with hot ethanol. The precipitate was filtered off. A red powder was obtained, 0.245 g, 65% yield; mp 196–200 °C. ^{1}H NMR ($CDCl_3$): δ 6.405 (ddd, 1H), 6.702 (s, 1H), 6.817 (td, 1H), 7.091–7.419 (m, 9H), 7.463 (td, 1H), 7.747 (dd, 1H), 7.786 (d, 1H), 8.009 (s, 1H), 8.057 (ddd, 1H), 8.136 (dd, 1H). ^{13}C NMR ($CDCl_3$): δ 58.09 (C-S), 64.91 (C-S), 117.66 (C-H), 120.08 (C-H), 123.16 (C-H), 124.01 (C-H), 125.30 (C-H), 125.96 (C-H), 126.34 (C-H), 126.48 (C-H), 126.73 (C-H), 126.99 (C-H), 127.77 (C-H), 128.02 (C-H), 128.48 (C-H), 130.03 (C-H), 130.10 (C-H), 130.17 (C-H), 130.21 (C-H), 132.05 (C), 133.33 (C), 135.21 (C), 135.39 (C), 138.63 (C), 138.93 (C), 139.05 (C), 140.62 (C), 140.79 (C), 143.34 (C). ^{77}Se NMR ($CDCl_3$): δ 390.32.

9-(11′*H*-Benzo[*b*]fluoren-11′-ylidene)-9*H*-selenoxanthene (16). To a stirred solution of dispirothiirane **32** (0.200 g, 0.407 mmol) in anhydrous benzene (20 mL), protected by a $CaCl_2$ tube, PPh_3 (0.117 g, 0.447 mmol) was added. After refluxing for 3 h, the mixture was cooled to rt, and the solvent was removed under reduced pressure. Trituration of the crude product in boiling ethanol gave a precipitate, which was filtered off. A yellow powder was obtained, 0.171 g, yield 75%; mp 240–242 °C. A sample for analysis was purified by column chromatography on dry silica gel using petrol ether–Et_2O 96 : 4 as eluent. ^{1}H NMR ($CDCl_3$): δ 7.013 (td, $^3J = 7.3$ Hz, $^3J = 6.9$ Hz, $^4J = 1.2$ Hz, 1H), 7.239–7.464 (m, 9H), 7.637 (s, 1H), 7.808–7.908 (m, 6H), 8.051 (s, 1H). ^{13}C NMR ($CDCl_3$): δ 117.09 (C-H), 120.13 (C-H), 125.27 (C-H), 125.36 (C-H), 125.74 (C-H), 126.42 (C-H), 126.57 (C-H), 126.66 (C-H), 126.90 (C-H), 127.24 (C-H), 127.33 (C-H), 127.81 (C-H), 128.60 (C-H), 129.16 (C-H), 129.24 (C-H), 129.44 (C-H), 131.18 (C), 131.27 (C-H), 131.49 (C-H), 132.51 (C), 133.46 (C), 133.59 (C), 133.63 (C), 136.44 (C), 138.67 (C), 138.71 (C), 138.82 (C), 138.98 (C), 139.40 (C), 140.75 (C). ^{77}Se NMR ($CDCl_3$): δ 397.76. UV/VIS (cyclohexane): $c = 1.176 \times 10^{-4}$ M, λ_{max}/nm (ε/M^{-1} cm^{-1}): 310 (25525), shoulder 400 (4148). Calc. for $C_{30}H_{18}Se$: C, 78.77; H, 3.96; Se, 17.26. Found: C, 78.20; H, 3.96; Se, 16.75%. MS, *m*/*z* (% molecular ion): 460.05924 (24%, $^{12}C_{30}H_{18}{}^{82}Se$, and/or $^{12}C_{29}{}^{13}CH_{17}{}^{82}Se$), 459.05956 (34%, $^{12}C_{29}{}^{13}CH_{18}{}^{80}Se$), 458.05740 (100%, $^{12}C_{30}H_{18}{}^{80}Se$, and/or $^{12}C_{29}{}^{13}CH_{17}{}^{80}Se$), 457.05904 (20%, $^{12}C_{29}{}^{13}CH_{18}{}^{78}Se$), 456.05908 (54%, $^{12}C_{30}H_{18}{}^{78}Se$), 455.05860 (24%, $^{12}C_{30}H_{17}{}^{78}Se$).

Dispiro[11*H*-benzo[*b*]fluorene-11,2′-thiirane-3′,9″-(9″*H*-telluroxanthene)] (33). Dispirothiirane **33** was obtained analogously to dispirothiirane **32** with some modifications. To a stirred solution of thioketone **23** [freshly prepared from ketone **21** (0.200 g, 0.649 mmol), Lawesson's reagent (0.134 g, 0.331 mmol), in dried benzene (30 mL)] in anhydrous benzene (50 mL) protected by a $CaCl_2$ tube, diazo derivative **30** (0.161 g, 0.660 mmol) was added. The reaction mixture was refluxed for 3 h; the color of the reaction mixture became wine-red. Work-up of the reaction mixture as described in the procedure for **32** gave **33**, a red powder, 0.205 g, 58% yield; mp 163–165 °C (dec.). ^{1}H NMR ($CDCl_3$): δ 6.252 (ddd, $^3J = 7.9$ Hz, $^4J = 1.7$ Hz, $^5J = 0.7$ Hz, 1H), 6.533 (s, 1H), 6.817 (td, $^3J = 7.9$ Hz, $^3J = 7.4$ Hz, $^4J = 1.2$ Hz, 1H), 7.046–7.101 (m, 2H), 7.229 (td, $^3J = 7.5$ Hz, $^4J = 1.1$ Hz, 1H), 7.266–7.281 (m, 2H), 7.351–7.422 (m, 2H), 7.445–7.491 (m, 2H), 7.581 (ddd, $^3J = 7.5$ Hz, $^4J = 1.3$ Hz, $^5J = 0.4$ Hz, 1H), 7.765 (ddd, $^3J = 7.6$ Hz, $^4J = 1.1$ Hz, $^5J = 0.7$ Hz, 1H), 7.799 (d, 1H), 8.033 (s, 1H), 8.092 (ddd, $^3J = 7.8$ Hz, $^4J = 1.4$ Hz, $^5J = 0.5$ Hz, 1H), 8.161 (ddd, $^3J = 7.7$ Hz, $^4J = 1.4$ Hz, $^5J = 0.5$ Hz, 1H). ^{13}C NMR ($CDCl_3$): δ 58.58 (C-S), 69.81 (C-S), 117.65 (C-H), 120.06 (C-H), 122.30 (C), 122.72 (C), 123.26 (C-H), 124.06 (C-H), 125.27 (C-H), 125.97 (C-H), 126.74 (C-H), 126.89 (C-H), 126.94 (C-H), 127.12 (C-H), 127.22 (C-H), 127.76 (C-H), 127.98 (C-H), 128.54 (C-H), 131.12 (C-H), 131.34 (C-H), 132.50 (C), 133.35 (C), 135.81 (C-H), 135.83 (C-H), 139.31 (C), 140.98 (C), 141.05 (C), 141.53 (C), 141.83 (C), 143.80 (C). ^{125}Te NMR ($CDCl_3$): δ 612.60.

9-(11′*H*-Benzo[*b*]fluoren-11′-ylidene)-9*H*-telluroxanthene (17). Compound **17** was obtained analogously to **16**. A solution of dispirothiirane **33** (0.120 g, 0.222 mmol), and PPh_3 (0.064 g, 0.244 mmol), in anhydrous benzene (30 mL) protected by a $CaCl_2$ tube, was refluxed for 25 h. Trituration of the crude product in boiling ethanol gave a precipitate, which was filtered off. A yellow powder was obtained, 0.073 g, yield 65%; mp 240–244 °C. ^{1}H NMR ($CDCl_3$): δ 6.993 (m, 2H), 7.210 (td, $^3J = 7.5$ Hz, $^4J = 1.5$ Hz, 1H), 7.260 (m, 1H), 7.285–7.332 (m, 2H), 7.342–7.421 (m, 5H, H$^{10'}$), 7.763–7.842 (m, 4H), 8.012–8.085 (m, 3H, H$^{5'}$). ^{13}C NMR ($CDCl_3$): δ 117.10 (C-H), 119.27 (C), 119.28 (C), 120.10 (C-H), 125.32 (C-H), 125.44 (C-H), 125.78 (C-H), 126.39 (C-H), 127.04 (C-H), 127.14 (C-H), 127.22 (C-H), 127.58 (C-H), 127.62 (C-H), 127.80 (C-H), 128.54 (C-H), 128.99 (C-H), 129.27 (C-H), 130.99 (C), 132.60 (C), 133.44 (C-H), 136.41 (C), 137.02 (C-H), 137.22 (C-H), 138.68 (C), 139.35 (C), 140.71 (C), 142.44 (C), 142.64 (C), 144.49 (C). ^{125}Te NMR ($CDCl_3$): δ 619.19. UV/VIS (cyclohexane): $c = 1.615 \times 10^{-4}$ M, λ_{max}/nm (ε/M^{-1} cm^{-1}): 377.5 (6796) shoulder; $c = 3.230 \times 10^{-5}$ M, λ_{max} (ε/M^{-1} cm^{-1}): 312.5 (38792).

9*H*-Thioxanthene-9-thione (31). The thioketone was prepared according to the literature[30] (yield 88%), mp 167–171 °C (lit.[30] mp 168 °C). ^{1}H NMR ($CDCl_3$): δ 7.413 (td, $^3J = 8.4$ Hz, $^3J = 6.6$ Hz, $^4J = 1.8$ Hz, 2H, H^2, H^7), 7.578–7.648 (m, 4H, H^4, H^5, H^3, H^6), 9.022 (ddd, $^3J = 8.3$ Hz, $^4J = 1.3$ Hz, $^5J = 0.5$ Hz, 2H, H^1, H^8). ^{13}C NMR ($CDCl_3$): δ 125.93 (C-H), 126.96 (C-H), 131.64 (C-H), 131.89 (C), 133.31 (C-H), 137.61 (C), 211.25 (C=S).

Dispiro[11*H*-benzo[*b*]fluorene-11,2′-thiirane-3′,9″-(9″*H*-thioxanthene)] (34). Dispirothiirane **34** was obtained analogously to dispirothiirane **32**. To a stirred solution of thioketone **31** (0.333 g, 1.434 mmol) in anhydrous benzene (15 mL) protected by a $CaCl_2$ tube, diazo derivative **30** (0.372 g, 1.537 mmol) was added. The reaction mixture was refluxed for 4 h; the color of the reaction mixture became black. Work-up of the reaction mixture as described in the procedure for **32** gave a red-orange powder, 0.476 g, 58% yield; mp 179–180 °C (dec). ^{1}H NMR ($CDCl_3$): δ 6.549 (ddd, $^3J = 7.8$ Hz, $^4J = 1.4$ Hz, $^5J = 0.5$ Hz, 1H, H^1), 6.845 (td, $^3J = 7.8$ Hz, $^3J = 7.4$ Hz, $^4J = 1.2$ Hz, 1H, H^3),

6.859 (s, 1H, H^{10}), 7.127–7.249 (m, 4H, H^{2}, $H^{5''}$ or $H^{4''}$, $H^{2''}$, $H^{7''}$), 7.282–7.427 (m, 5H, $H^{3''}$, H^{9} or H^{6}, H^{8} or H^{7}, H^{7} or H^{8}, $H^{4''}$ or $H^{5''}$), 7.472 (td, ^{3}J = 7.7 Hz, ^{3}J = 7.2 Hz, ^{4}J = 1.5 Hz, 1H, $H^{6''}$), 7.748 (ddd, ^{3}J = 7.6 Hz, ^{4}J = 1.1 Hz, ^{5}J = 0.5 Hz, 1H, H^{4}), 7.792 (dd, ^{3}J = 8.1 Hz, ^{5}J = 0.7 Hz, 1H, H^{6} or H^{9}), 8.011 (s, 1H, H^{5}), 8.060 (ddd, ^{3}J = 7.7 Hz, ^{4}J = 1.4 Hz, ^{5}J = 0.5 Hz, 1H, $H^{1''}$), 8.145 (ddd, ^{3}J = 7.7 Hz, ^{4}J = 1.4 Hz, ^{5}J = 0.5 Hz, 1H, $H^{8''}$). ^{13}C NMR ($CDCl_3$): δ 57.73 (C-S), 62.23 (C-S), 117.73 (C-H), 120.12 (C-H), 123.26 (C), 123.29 (C), 124.12 (C-H), 126.71 (C-H), 126.98 (C-H), 127.63 (C-H), 127.70 (C-H), 127.80 (C-H), 128.07 (C-H), 128.46 (C-H), 129.20 (C-H), 129.36 (C-H), 132.55 (C-H), 133.42 (C), 137.70 (C), 137.72 (C), 137.79 (C), 137.99 (C), 138.97 (C), 140.36 (C), 140.76 (C), 143.10 (C).

9-(11′*H*-Benzo[*b*]fluoren-11′-ylidene)-9*H*-thioxanthene (18). (a) Compound **18** was obtained analogously to **16**. A solution of dispirothiirane **34** (0.150 g, 0.393 mmol), and PPh_3 (0.102 g, 0.389 mmol), in anhydrous benzene (30 mL) protected by a $CaCl_2$ tube, was refluxed for 8 h. Trituration of the crude product in boiling ethanol gave a precipitate, which was filtered off. A red powder was obtained, 0.156 g, yield 97%; mp 229 °C.

(b). To a stirred solution of dispirothiirane **34** (0.050 g, 0.113 mmol) in anhydrous xylene (10 mL) protected by a $CaCl_2$ tube, copper bronze (0.035 g) was added. The reaction mixture was refluxed for 5 h. After cooling, the black precipitate was filtered off and washed with CH_2Cl_2. The xylene was evaporated *in vacuo*. Column chromatography of the crude product was performed on dry silica gel using the eluent petrol ether–Et_2O 98 : 2. The color of **18** on the column was yellow; it was eluted first. It was obtained as a yellow-red powder. Final purification was performed with sublimation at 240 °C/0.1 mmHg. Mp 229 °C. ^{1}H NMR ($CDCl_3$): δ 7.041 (td, ^{3}J = 8.1 Hz, ^{3}J = 7.3 Hz, ^{4}J = 1.2 Hz, 1H, $H^{2'}$), 7.314–7.420 (m, 6H, H^{6}, H^{7}, H^{3}, H^{2}, $H^{7'}$, $H^{3'}$), 7.430–7.484 (m, 2H, $H^{1'}$, $H^{8'}$), 7.500 (br d, ^{3}J = 8.1 Hz, 1H, $H^{6'}$), 7.739 (m, 1H, H^{4}), 7.787 (m, 1H, H^{5}), 7.832 (s, 1H, $H^{10'}$), 7.867 (m, 3H, H^{1}, $H^{4'}$, $H^{9'}$), 7.933 (m, 1H, H^{8}), 8.068 (s, 1H, $H^{5'}$). ^{13}C NMR ($CDCl_3$): δ 117.07 (C-H), 120.14 (C-H), 125.14 (C-H), 125.38 (C-H), 125.69 (C-H), 126.01 (C-H), 126.11 (C-H), 126.43 (C-H), 126.78 (C-H), 127.26 (C-H), 127.37 (C-H), 127.82 (C-H), 128.61 (C-H), 128.72 (C-H), 128.85 (C-H), 128.95 (C-H), 128.13 (C-H), 129.23 (C-H), 131.29 (C), 132.47 (C), 133.49(C), 135.88 (C), 136.50 (C), 136.73 (C), 136.80 (C), 137.37 (C), 137.48 (C), 138.76 (C), 139.48 (C), 140.80 (C). UV/VIS (cyclohexane): $c = 3.268 \times 10^{-5}$ M, λ_{max}/nm (ε/M^{-1} cm^{-1}): 316.1 (13494), 348.3 (7772), 450.7 (1774).

References

1 G. Shoham, S. Cohen, R. M. Suissa and I. Agranat, in *Molecular Structure: Chemical Reactivity and Biological Activity*, J. J. Stezowski, J.-L. Huang and M.-C. Shao, Eds., Oxford University Press, Oxford, 1988, p. 290.
2 J. Sandström, in *The chemistry of double-bonded functional groups, Supplement A3*, S. Patai, Ed., Wiley, New York, 1997, p. 1253.
3 P. U. Biedermann, J. J. Stezowski and I. Agranat, in *Advances in Theoretically Interesting Molecules*, Vol. 4, R. P. Thummel, Ed., JAI Press, Stamford, CT, 1998, p. 245.
4 P. U. Biedermann, J. J. Stezowski and I. Agranat, *Eur. J. Org. Chem.*, 2001, 15.
5 P. U. Biedermann, J. J. Stezowski and I. Agranat, *Chem. Commun.*, 2001, 954.
6 P. U. Biedermann, A. Levy, J. J. Stezowski and I. Agranat, *Chirality*, 1995, **7**, 199.
7 W. Luef and R. Keese, *Top. Stereochem.*, 1991, **20**, 231.
8 Y. Tapuhi, M. R. Suissa, S. Cohen, P. U. Biedermann, A. Levy and I. Agranat, *J. Chem. Soc., Perkin Trans. 2*, 2000, 93.
9 B. L. Feringa, W. F. Jager and B. de Lange, *Tetrahedron Lett.*, 1992, **33**, 2887.
10 N. A. Bailey and S. E. Hull, *Acta Crystallogr., Sect. B*, 1978, **34**, 3289.
11 J.-S. Lee and S. C. Nyburg, *Acta Crystallogr., Sect. C*, 1985, **41**, 560.
12 J. F. D. Mills and S. C. Nyburg, *J. Chem. Soc.*, 1963, 308.
13 E. Harnik and G. M. J. Schmidt, *J. Chem. Soc.*, 1954, 3295.
14 K. S. Dichmann, S. C. Nyburg, F. H. Pickard and J. A. Potworowski, *Acta Crystallogr., Sect. B*, 1974, **30**, 27.
15 I. Agranat and Y. Tapuhi, *J. Am. Chem. Soc.*, 1978, **100**, 5604.
16 I. Agranat and Y. Tapuhi, *J. Am. Chem. Soc.*, 1979, **101**, 665.
17 I. Agranat and Y. Tapuhi, *J. Org. Chem.*, 1979, **44**, 1941.
18 B. L. Feringa, A. M. Schoevaars, W. F. Jager, B. de Lange and N. P. M. Huck, *Enantiomer*, 1996, **1**, 325.
19 A. Levy, P. U. Biedermann, S. Cohen and I. Agranat, *J. Chem. Soc., Perkin Trans. 2*, 2000, 725.
20 A. Levy, P. U. Biedermann and I. Agranat, *Org. Lett.*, 2000, **2**, 1811.
21 *Reason and Imagination: Reflections on Research in Organic Chemistry: Selected Papers of Derek H. R. Barton*, D. H. R. Barton, Ed., Imperial College Press and World Scientific, Singapore, 1996, vol. 6, p. 489.
22 D. H. R. Barton and B. J. Wills, *J. Chem. Soc., Perkin Trans. 1*, 1972, 305.
23 D. H. R. Barton, F. S. Guziec and I. Shahak, *J. Chem. Soc., Perkin Trans. 1*, 1974, 1794.
24 R. Lesser and R. Weiß, *Ber. Dtsch. Chem. Ges.*, 1914, **47**, 2510.
25 K. Šindelàr, E. Svàtek, J. Metyošovà, J. Metys and M. Protiva, *Collect. Czech. Chem. Commun.*, 1969, **34**, 3792.
26 I. D. Sadekov and V. I. Minkin, *Adv. Heterocycl. Chem.*, 1995, **63**, 1.
27 I. D. Sadekov, A. A. Ladatko and V. I. Minkin, *Khim. Geterotiskl. Soedin.*, 1980, 1342.
28 S. Scheibye, R. Shabana and S.-O. Lawesson, *Tetrahedron*, 1982, **38**, 993.
29 M. P. Cava and M. I. Levinson, *Tetrahedron*, 1985, **41**, 5061.
30 B. S. Pedersen, S. Scheibye, N. H. Nilsson and S.-O. Lawesson, *Bull. Soc. Chim. Belg.*, 1978, **87**, 223.
31 A. Schoenberg, W. I. Awad and N. Latif, *J. Chem. Soc.*, 1951, 1368.
32 P. U. Biedermann, A. Levy, M. R. Suissa, J. J. Stezowski and I. Agranat, *Enantiomer*, 1996, **1**, 75.
33 K. J. Irgolic, in *Methods of Organic Chemistry Houben-Weyl, Vol. E12b, Organotellurium Compounds*, D. Klamann, Ed., Georg Thieme Verlag, Stuttgart, 1990, p. 830.
34 I. L. Karle and J. Karle, in *Organic selenium compounds: their chemistry and biology*, D. L. Klayman and W. H. H. Günther, Eds., Wiley-Interscience, London, 1973, p. 989.
35 A. Latif and G. Soliman, *J. Chem. Soc.*, 1944, 56.
36 W. F. Jager, B. de Lange, A. M. Schoevaars, F. van Bolhuis and B. L. Feringa, *Tetrahedron: Asymmetry*, 1993, **4**, 1481; E. M. Geertsema, A. Meetsma and B. L. Feringa, *Angew. Chem.*, 1999, **111**, 2902.
37 Y. V. Zefirov, *Crystallogr. Rep.*, 1997, **42**, 111.
38 A. Bondi, *J. Phys. Chem.*, 1964, **68**, 441.
39 A. S. Antsyshkina, A. I. Uraev, O. I. Dimitrieva, A. D. Garnovskii and I. D. Sadekov, *Zh. Neory. Khim.*, 1998, **43**, 438; Cambridge Structural Database, Structure NUMMIR; F. H. Allen and O. Kenard, *Chem. Des. Autom. News*, 1993, **8**, 1; F. H. Allen and O. Kenard, *Chem. Des. Autom. News*, 1993, **8**, 31.
40 A. Levy, P. U. Biedermann, S. Cohen and I. Agranat, *Phosphorus, Sulfur Silicon Relat. Elem.*, 1998, **136–138**, 139.
41 J. J. P. Stewart, *J. Comput. Chem.*, 1989, **10**, 221; J. J. P. Stewart, *J. Comput. Chem.*, 1991, **12**, 320.
42 J. J. P. Stewart, MOPAC 6.00, QCPE 455, Frank J. Seiler Research Laboratory, United States Air Force Academy, Colorado Springs, CO, USA, 1990.
43 W. Nakanishi, Y. Yamamoto, S. Hayashi, H. Tukada and H. Iwamura, *J. Phys. Org. Chem.*, 1990, **3**, 369.
44 G. M. Sheldrick, in *Crystallographic Computing*, Vol. 3, Oxford University Press, Oxford, 1985, p. 175.
45 P. B. Grasse, J. J. Zupancic, S. C. Lapin, M. P. Hendrich and G. B. Schuster, *J. Org. Chem.*, 1985, **50**, 2352.
46 W. F. Jager, PhD Thesis, Rijksuniversiteit Groningen, 1994, The Netherlands.